UPTEC X 03 021
MAY 2003
ISSN 1401-2138

ELIN CEDERHOLM

Improved liquid exchange rate and resolution of fast interactions using SPR-technology

Master’s degree project

UPPSALA UNIVERSITET

Molecular Biotechnology Programme

Uppsala University School of Engineering

UPTEC X 03 021	**Date of issue 2003-05**

Author

Elin Cederholm

Title (English)

Improved liquid exchange rate and resolution of fast interactions using SPR-technology

Title (Swedish)

Abstract

The resolution of fast interactions with Biacore technology is partly limited by the flow system and the liquid exchange rate. By improving the liquid exchange rate, the shift between buffer and sample in the flow cell can be done faster, minimizing sample dispersion and the so-called rise and fall times are shortened. New injection principles for fast interactions were implemented and evaluated. Both the lane shift and stealth inject uses the principle of hydrodynamic addressing to introduce the sample flow in the flow cell before the injection start. In the currently used Biacore S51, six times faster rise times was obtained with the stealth inject. With the new flow cell PSI and the lane shift, the rise times were improved ten times, which means that ten times faster interactions can be measured. The largest improvement was seen for low flow rates. The fall times were slightly improved or unchanged.

Keywords

Biacore, SPR-technology, hydrodynamic addressing, kinetics, rise and fall times

Supervisors

Mattias Tidare
Biacore AB, Uppsala

Scientific reviewer

Stefan Löfås
Biacore AB, Uppsala

Project name	Sponsors
Language **English**	Security
ISSN 1401-2138	Classification
Supplementary bibliographical information	Pages **38**

Biology Education Centre Biomedical Center Husargatan 3 Uppsala
Box 592 S-75124 Uppsala Tel +46 (0)18 4710000 Fax +46 (0)18 555217

IMPROVED LIQUID EXCHANGE RATE AND RESOLUTION OF FAST INTERACTIONS USING SPR-TECHNOLOGY

ELIN CEDERHOLM

SAMMANFATTNING

En BIACORE är ett analysinstrument som används för att mäta t.ex. hur snabbt eller starkt två molekyler binder till varandra. Den ena molekylen fästs på en yta i en flödescell inuti i instrumentet och den andra molekylen (provet) sugs upp från ett provrör via en spruta för att sedan injiceras med ett kontinuerligt flöde i flödescellen. När molekylerna binder till varandra resulterar det i att massan nära ytan ökas. Massökning mäts med ytplasmonresonans och översätts sedan till hastighet (kinetik) och styrka (affinitet) i bindningen.

Hur snabba bindningar (interaktioner) man kan mäta med en BIACORE begränsas till stor del av provdispersion (provet späds ut i bufferten) i vätskesystemet. Detta ger en tidsfördröjning innan provet når 100 % respektive 0 % provkoncentration i flödescellen, s.k. stig- och falltider. I det här projektet har nya injektionsprinciper och flödessystem för snabbare skift mellan buffert och prov i flödescellen testats. Ett snabbare skift gör att tiden för provdispersion minskas och stig- och falltiderna kortas, vilket i sin tur leder till att snabbare interaktioner kan mätas. Genom att smyga in provet i flödescellen innan injektionsstarten kunde stigtiderna förbättras mellan 6-10 ggr, vilket betyder att 6-10 ggr snabbare interaktioner kan mätas. Att kunna mäta snabbare interaktioner mellan molekyler är framförallt intressant inom läkemedelsutveckling.

Examensarbete 20 p i Molekylär Bioteknikprogrammet

Uppsala Universitet, Maj 2003

Table of Contents

1 INTRODUCTION

Detailed kinetic information with both affinity data and separate measurement of the association and dissociation rates for small molecules provides valuable information for lead optimization, hit selection and early ADME (adsorption, distribution, metabolism and excretion) studies in drug discovery. The binding affinity (K_D), between a candidate drug and its target is a function of the association (k_a) and dissociation rate (k_d) according to $K_D=k_d/k_a$. Two compounds displaying similar affinities for a target molecule may have significantly different binding and dissociation rates, factors that can be important in determining drug efficacy. Kinetic rate constants are also important in kinetic based QSAR (quantitative structure-activity relationship), providing more information on structural activity relationships. A structural variation of a compound that results in the same affinity can still have an effect on the functional activity as the binding rate and dissociation rate may vary with several orders of magnitude [1, 2]. Measurements of the kinetic rate constants are also of great interest in the life science area for the characterization of fast interactions involved in for example signal transduction or other biological systems.

Biacore uses surface plasmon resonance (SPR) biosensor technology to study biomolecular interactions in real time. One interactant (ligand) is immobilized on a sensor surface and the other interactant (analyte) is passed over the surface in a continuous flow. When the analyte binds to the ligand, the surface mass concentration increases and the refractive index is changed. The change in refractive index is monitored by the SPR detector and the resulting binding curve can be used to determine kinetic parameters of the interaction. Information on both the affinity and association and dissociation rate constants can be obtained.

Today association rate constants ranging from $1*10^3$ - $5*10^6$ [$M^{-1}s^{-1}$] and dissociation rate constants between $1*10^{-1}$ - $5*10^{-6}$ [s^{-1}] can be resolved with Biacore. The range of rate constants that can be resolved is linked to the design of the sample delivery system, to the concentration of the immobilized target and to the sensitivity of the detection [3]. To be able to measure fast interactions, it is crucial that the exchange of buffer with sample occurs fast enough, i.e. a high liquid exchange rate [4]. Improving the present range of rate constants that can be resolved would help characterize fast interaction that cannot be resolved today. Furthermore, it would be possible to resolve a greater range of affinity data in separate measurements of association and dissociation rate constants, providing valuable information in both lead optimization and kinetic based QSAR.

One of the factors limiting the resolution of fast kinetic parameters is dispersion of the sample in the sample delivery system. At the beginning and end of an injection the concentration of the sample is diluted by dispersion, i.e. mixing of the sample with running buffer. This gives rise to a short time lag for the concentration rise and fall, the so-called rise and fall times. With a faster liquid exchange rate, i.e. the time it takes to replace the running buffer with sample, the time for dispersion to occur will be minimized giving shorter rise and fall times and improved resolution of fast interactions [4]. The liquid exchange rate can be improved by increasing the flow rate and by minimizing the dead volume between sample and detection spot and between detection spot and running buffer. The time resolution can also be limited by

the sampling rate of the detector and therefore the sampling rate must be adjusted to a high enough rate to resolve the interactions.

In this report, the aim was to increase the resolution of fast interactions by testing new injection methods for an improved liquid exchange rate. With an improved liquid exchange rate, dispersion is reduced and the rise and fall times shortened. This report concentrates on the rise and fall times measured for different flow cells and injection methods. The performance of a new flow cell, called the PSI cell, was tested. With the prototype 3D-PSI flow cell the rise times could be improved on average 10 times. In the PSI cell it is possible to introduce the sample flow in the flow cell before the injection start as a defined sample lane by means of hydrodynamic addressing. At the injection start the sample lane is moved to the detection spot by adjusting the relative flow rates of the buffer pumps. The time for dispersion to occur is limited to the time it takes to move the sample lane, which is only a fraction of the time it takes to fill the flow cell, and the rise time is shortened. With the stealth inject described in this report, the rise times in the so-called Y-cell in Biacore S51 could be improved by on average a factor six. The effect on the rise and fall times for different diffusion coefficients was also studied. Kinetic determination of low molecular weight compounds interacting with human serum albumin (HSA) using the lane shift in the PSI cell was also performed.

2 THEORETICAL BACKGROUND

2.1 BIACORE TECHNOLOGY

2.1.1 Sensor surface

The surface of a sensor chip consists of three layers: glass, a thin gold film, and a matrix layer. The matrix is covalently bound to the gold film through an inert linker layer. The most versatile sensor chip, Sensor Chip CM5, has a carboxymethyl dextran hydrogel and can be used for most applications.

Besides providing a hydrophilic environment, the hydrogel also allows for covalent immobilization of bio-molecules, increases the sensitivity by increasing the binding capacity of the surface and provides a very low degree of non-specific binding to the surface. The metal layer is necessary for the generation of the SPR signal and gold is chosen since it gives a good SPR response and is chemically inert to the solvents and solutes typically used [5].

The sensor chip forms one wall of the micro-flow cell, with the hydrogel-covered side coming in contact with the solution being studied. The gold film is illuminated from the other side, giving rise to SPR.

2.1.2 SPR detection

Biacore uses surface plasmon resonance, SPR, to detect interactions in real-time. When light comes from a medium of higher refractive index (such as glass) to a medium of lower refractive index (water), the light is partly reflected and partly refracted. Above a critical angle of incidence, total internal reflection occurs and no light is refracted across the interface. There is however still an electromagnetic field component, called the evanescent wave that penetrates a short distance into the medium of lower refractive index. If the interface is coated with a thin metal film, like the gold film in Biacore, and the light is monochromatic and p-polarised [1], surface plasmon resonance can be observed as markedly reduced intensity of the reflected light occurring at a specific angle called the SPR angle [5].

The SPR angle is effected by the properties of the metal film, the wavelength of the incident light and the refractive index of the media on either side of the metal film. In Biacore instruments, all but the refractive index of the less dense media (here the aqueous layer adjacent to the gold surface), are kept constant, and SPR is used to detect changes in the refractive index of the aqueous layer immediately adjacent to the gold surface. As the composition and concentration of the solute changes, the refractive index changes and hence also the SPR angle.

By monitoring the SPR angle, a real-time measure of changes in the mass concentration is provided. The SPR signal is expressed in resonance units (RU) and a change in the signal of 1000 RU corresponds to a change in surface concentration of about 1 ng/mm^2 for most biomolecules [5]. The response is plotted against time and presented in a so called sensorgram.

[1] i.e. the electric vector component of the light is parallel to the plane of incident

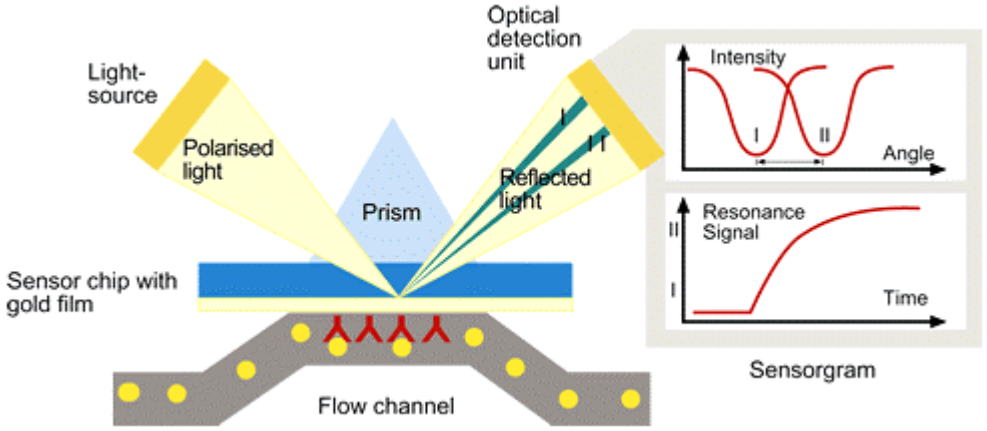

Figure 1 Illustration the SPR technology. Binding of analyte to the sensor surface (via coupled antibodies) increases the refractive index and the SPR angle is changed which generates a signal (change in resonance angle, SPR angle I ? SPR angle II). The resonance signal is monitored and plotted over time, forming the sensorgram. Illustration used with permission from Biacore.

2.1.3 Flow system

Biacore uses an integrated micro-fluidic flow system to deliver buffer and sample to the sensor surface in a continuous flow. When a sensor chip is inserted in the instrument, it is docked against a so-called integrated μ-fluidic cartridge (IFC), with the sensor surface forming one wall of the flow cell and precision grooves in the IFC surface forming the other three walls. The IFC is made up of a series of precision-cast channels in a hard polymer plate, forming sample loops and flow channels for buffer and sample delivery. The IFC controls the delivery of samples and buffers to the sensor chip surface and the liquid flow is directed through the required channels by IFC valve operations. Details of IFC design vary between different instruments. The valves in the IFC are pneumatic micro-valves automatically controlled through the instrument software [5].

The switch between buffer and sample is almost instantaneous, so the sample is delivered to the sensor surface as a defined liquid segment with minimum dispersion and accurate control of sample contact time. With continuous flow the concentration of free analyte is constant and therefore known at all times.

In fully automated systems, two motor-driven syringe pumps are used, one which injects the samples in defined volumes from the autosampler to the IFC (dispensor-pump) and one which provides a continuous flow of buffer through the IFC (flow-pump).

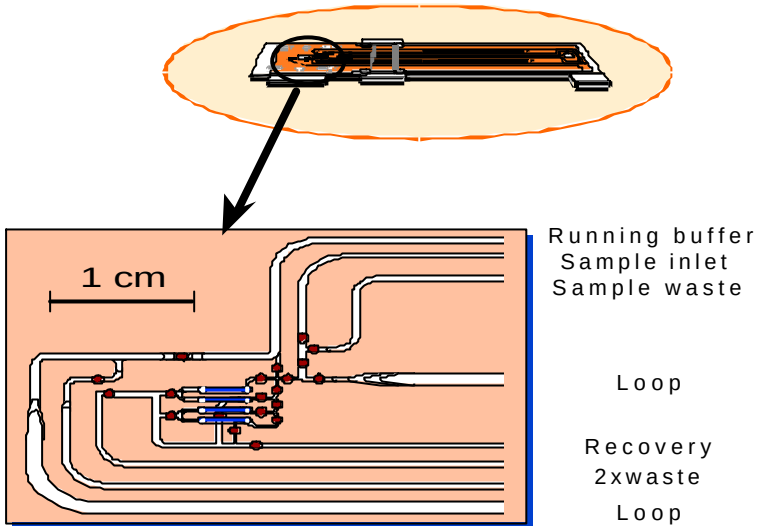

Figure 2 Schematic illustration of the IFC in BIACORE 3000. Illustration used with permission from Biacore.

2.1.4 Flow cell design

The flow cell design varies between different instruments. In BIACORE 3000 there are four different flow cells, which can be used individually or serially for simultaneous analysis (figure 3a). The dimensions of each flow cell in BIACORE 3000 is 0.5×2.4×0.02 mm, and the volume 0.02 µl with a sensing area of 1.2 mm^2. The dead volume[2] from the inlet valve to the first flow cell is 0.5 µl and the dead volume between flow cells is 0.3 µl [6]. By simultaneous measurements of the flow cells, direct automatic reference subtraction is allowed.

Biacore S51 has two flow cells but only one can be used at a time. The flow cells in Biacore S51 are called Y-cells or HA-cells. The dimension is approximately 0.9×2.9×0.04 mm, and the volume is ~0.1 µl with a sensing area of 2.61 mm^2. Each flow cell has three independent detection spots arranged transversely across the flow cell (see figure 3b) that ensures that the access of sample to all spots is essentially simultaneous. The spot in the middle is used as a reference spot while the two outer spots are used for ligand immobilization. The flow cell has two inlets and one common outlet and during the immobilization the spots are selected by adjusting the relative flow rates from the two inlets. This is called hydrodynamic addressing [7].

Biacore prototype 3D-PSI has only one flow cell, called the PSI-cell. It has three inlets and one common outlet (figure 3c). Two inlets are used for buffer and one inlet for sample and by means of hydrodynamic addressing up to as many as 11 spots may be addressed separately. The dimension of the prototype PSI-cell is approximately 1.5×2.9×0.05 mm, with a volume of ~0.2 µl and surface area of 4.35 mm^2 [8].

[2] i.e. the volume where dispersion occurs

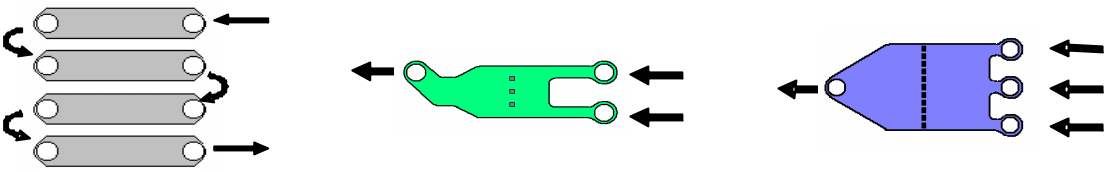

A) Biacore 3000 B) Y-cell Biacore S51 C) PSI-cell

Figure 3 Schematic picture of the flow cells, a) showing the flow cells in BIACORE 3000, b) the so-called Y-cell in Biacore S51 and c) the PSI-cell. The black dots represent the detection spots in the flow cells.

2.2 KINETIC MEASUREMENTS WITH BIACORE

By monitoring the SPR response, changes in refractive index close to the sensor surface is detected and binding interactions between molecules can be detected in real-time without any labelling requirements. One interactant, referred to as the ligand, is immobilized on the sensor surface, while the other interactant, called the analyte, is passed over the surface in a continuous flow [9].

A typical kinetics run consists of four phases; 1) the establishment of a stable baseline with running buffer, 2) association phase, i.e. injection of sample dissolved in running buffer, 3) equilibrium and 4) dissociation phase, i.e. wash out with running buffer, figure 4 [1]. By fitting the resulting binding data presented in the sensorgrams to mathematical models describing the interaction kinetic rate constants and affinity constants can be determined.

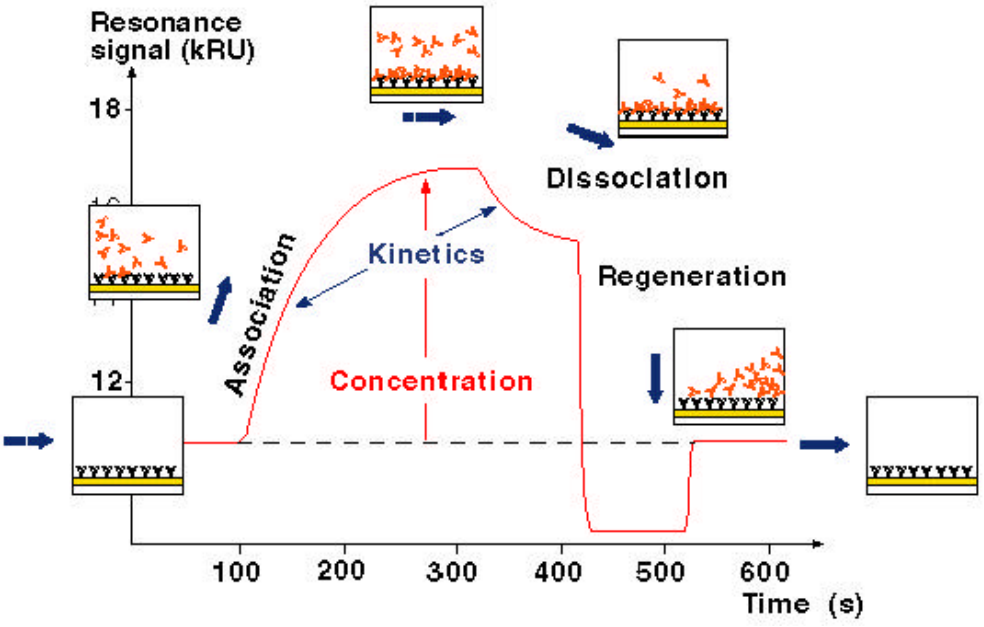

Figure 4 Schematic representation of a kinetic run in Biacore. Illustration used with permission from Biacore.

A reference surface is needed to correct for differences in refractive indexes between the sample and buffer and to subtract systematic disturbances. By subtracting the

response of the reference surface from the response of the ligand surface, the measured response during sample injection correctly reflects the amount of analyte bound.

The kinetic rate equation for a bimolecular interaction is described by:

$d[AB]/dt = k_a[A][B] - k_d[AB]$

where [AB] is the concentration of formed complex, [A] concentration of free analyte, and [B] the ligand concentration, k_a is the association rate constant and k_d is the dissociation rate constant. At equilibrium, equal number of complex forms and dissociates and $d[AB]/dt = 0$, and the equilibrium constants are described by:

$K_D = [A][B]/[AB]$ or $K_D = k_d/k_a$ (dissociation equilibrium constant [M])

$K_A = [AB]/[A][B]$ or $K_A = k_a/k_d$ (association equilibrium constant [M^{-1}])

With SPR detection the measured increase in response, R, is related to the increase in surface mass concentration and the number of complexes formed. The association phase is described by

$dR/dt = k_aC(R_{max} - R) - k_dR$

and at equilibrium the response is obtained as

$R_{eq} = k_aCR_{max}/(k_aC + k_d)$

and during dissociation

$dR/dt = - k_dR$

where R signifies the response at any time t, R_{eq} the response at equilibrium and R_{max} the maximum binding capacity of the surface in RU. C is the molar concentration of the analyte [5]. From the expressions above it is seen that the association phase depends on the association and dissociation rate constants, as well as the concentration of the analyte, whereas the dissociation phase only depends on the dissociation rate constant.

2.2.1 Kinetic determination of low-molecular weight compounds

As the SPR response is related to the change in surface *mass* concentration, the response depends on the molecular weight of the analyte. Analytes with low molecular weight will therefore give a low response, especially if the number of ligand sites is low. Bulk effects are corrected for by subtracting the response of a blank reference spot from the response of the ligand spot. But because the bulk solution is excluded from the volume occupied by ligand molecules on the ligand spot, the bulk contribution to the relative response is smaller on the detection spot than on the reference spot, and hence, reference subtraction does not exactly correct for bulk effects.

In the case of low molecular analytes, the contribution from the bulk effect can be in the same order of magnitude as the binding response (typically of the order of 50-100 RU or less). A small difference between the buffer and sample composition will give different reference subtraction error during sample injection and the relative response will be incorrect.

Low molecular weight samples are often dissolved in buffer containing DMSO for solubility reasons, and since DMSO give a significant contribution to the refractive index, a small variation in DMSO concentration between samples and running buffer can give a relatively large bulk effect. This results in large errors in relative response values and the response from the binding of the analyte is difficult to detect. To avoid these problems, solvent correction can be used. A solvent correction curve is established by injecting solvent correction solutions with known DMSO-content [10].

2.3 LIMITING FACTORS OF THE RESOLUTION OF FAST INTERACTIONS

2.3.1 Rise and fall times/Dispersion

The resolution of fast interactions in Biacore is today mainly limited by the liquid exchange rate. For kinetic measurements, it is important for the sample to be delivered to the sensing area in a defined volume with minimal dispersion. At the start and end of an injection, the sample concentration is diluted by dispersion i.e. the sample is mixed with running buffer in the injection system. This gives rise to a time lag in both the rise and fall of the response in the sensorgram, referred to as the "rise and fall times" (fig 5). These rise and fall times limits the resolution of fast kinetics, i.e. kinetic processes with short kinetic time constants [4].

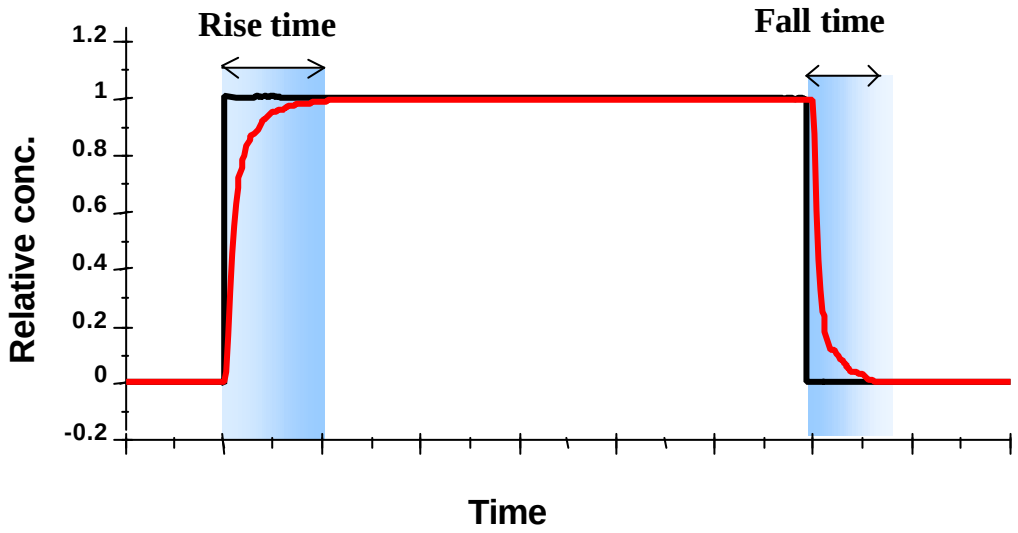

Figure 5 Illustration of the rise and fall times. The black line represents the ideal situation and the red curve the actual situation.

The sample is delivered to the sensor surface in a sample "plug". A few alternating air and sample segments are aspirated and injected into the IFC, the front segments[3] primes the injection channel and leaves via the waste. Air segments at the end of the sample plug act as diffusion and convective barriers, thus minimising dispersion at the sample end. Both leading dispersion and trailing dispersion, corresponding to rise and fall times, are dominated by the dead volume between the flow cell and the injection channel. The dead volume is the volume the sample has to travel before reaching the detection spot.

A 1:st order kinetic process can be used as a first approximation to describe the dispersion [4]:

$$\frac{dC}{dt} = k_{Dsp} \cdot (C_0 - C) \quad \text{or}$$

$$\frac{d\frac{C}{C_0}}{dt} = k_{Dsp} \cdot \left(1 - \frac{C}{C_0}\right) \qquad \text{(Eq.1)}$$

where k_{Dsp} is the dispersion rate constant, C_0 is the analyte concentration [M] and C is the analyte concentration at the sensor surface.

Analytical expressions for the concentration time course during rise (Eq.2a) and fall (Eq.2b) time are given by integrating Eq.1:

$$\frac{C}{C_0} = 1 - e^{-k_{Dsp} \cdot t} \qquad \text{(Eq.2a)}$$

$$\frac{C}{C_0} = e^{-k_{Dsp} \cdot t} \qquad \text{(Eq.2b)}$$

An expression for the time delay during rise and fall can be derived from these equations:

$$t_{delay} = -\frac{\ln(E)}{k_{Dsp}} \qquad \text{(Eq.3)}$$

where $E=1-C/C_0$ for the rise time and $E= C/C_0$ for the fall time. Defining the rise time as the time to reach 99 % of the final value (C_0) and the fall time as the time for the response to fall down to 1 %, k_{Dsp} can be calculated as follows if the rise and fall times are measured:

$$\frac{C}{C_0} = 0.99 \Rightarrow E = 1 - 0.99 = 0.01 \Rightarrow \quad k_{Dsp} = \frac{4.6}{t_{rise}}$$

The larger k_{Dsp}, is the shorter rise and fall times will be and the faster reactions can be resolved. Since the dispersion rate constant is approximately proportional to the

[3] Front segments are only used in Biacore 3000.

flow rate and inversely proportional to the dead volume, increasing the flow rate or minimising the dead volume can increase the resolution of fast interactions [4]. However, increased flow rate will give shorter rise and fall times at the cost of higher sample consumption.

2.3.2 Mass transport

Another limitation of measuring fast interaction rates is the so-called mass transport. Mass transport relates to the speed at which molecules can be transported to and from a surface. In Biacore, one interactant is immobilized to the surface and the other interactant has to diffuse from the bulk to the surface to bind. If the reaction between the analyte and ligand occurs at a higher rate than the transport of analyte to the surface, the reaction is said to be mass transport limited. Measurements under mass transport limitations will give an incorrect measurement of the reaction rate. During the dissociation phase, rebinding will occur if the reaction rate is faster than the transport rate and the apparent dissociation rate constant will be lower than the actual. Mass transport may be represented as follows [9]:

$$A_0 \underset{km}{\overset{km}{\rightleftarrows}} A_S + B \underset{kd}{\overset{ka}{\rightleftarrows}} AB$$

where k_m is the mass transport rate constant, which describes the flux of molecules to the sensor surface and out from the sensor surface (k_m will be the same in both directions), and k_a is the association rate constant and k_d is the dissociation rate constant. A_0 is the concentration of the injected sample and A_S is the surface concentration of A.

When the reaction rate is entirely mass transport limited, the sensor surface can be seen as an infinite sink and the concentration of A at the surface will be zero. In this case k_m can be described by:

$$k_m = 0.98\left(\frac{D}{h}\right)^{2/3}\left(\frac{f}{b \cdot x}\right)^{1/3}$$

where D is the diffusion coefficient, h and b are the flow cell height and width, f is the volumetric flow and x is the distance from the flow cell entrance [9].

The mass transport rate, k_m, depends of the diffusion rate of the analyte, the buffer flow and the shape and size of the flow cell. Increasing the flow rates and using low immobilization levels can reduce the mass transport effect.

2.3.4 Diffusion

When two fluids are in contact with each other diffusion will occur. At first, the concentration difference can be describes as a step function. As time passes, the diffusion will increase and a concentration gradient is formed. The contact time and the characteristics of the molecule will determine the diffusion. The contact time is determined by the distance to the detector and the linear flow rate, which is effected by the flow cell width and length. A low flow rate gives a longer contact time and

increased diffusion. The shape, size and viscosity of the molecule will effect the diffusion; a small molecule will diffuse faster than a large molecule. The diffusion coefficient of a molecule is also temperature dependent and the diffusion increases with increasing temperature. The diffusion occurs across the interface and the diffusion distance is defined as the distance from the interface to 1% in the concentration gradient [8].

2.3.5 Sampling rate/ Time resolution

The SPR-response is monitored in real-time. A fixed array of light-sensitive diodes covers the whole wedge of reflected light from the sensor. The signals from the diode detectors are analysed and the angle at which minimum reflection occurs is calculated by computer interpolation [5]. By increasing the sampling rate of the detector, the sample period is shortened and the time resolution increased, and faster reactions can be monitored.

Increasing the sampling rate will however result in a higher noise level, and in the case of kinetic analysis with low ligand density, the detector/electronic noise is often limiting. It is important to have a signal level larger than the detection limit, often defined as a signal larger than three times the standard deviation of the noise [11]. When analysing low molecular compounds it is especially important with a low noise level since the response in general is low.

2.4 HYDRODYNAMIC ADDRESSING

2.4.1 Principle of hydrodynamic addressing

The principle of hydrodynamic addressing (HA) uses laminar flow techniques to position the flow on the sensing area. A flow cell with two (three) separate inlets and a common outlet is used and by varying the flow rates at the inlets, the liquid can be directed to different "lanes" in the flow cell. The position of the liquid interface between the flows is determined by the relative flow rates [12].

The basic condition for hydrodynamic addressing is for the flow to be laminar. The type of flow depends on the linear flow rate, the viscosity of the liquid and the geometry of the pipe or flow cell. Reynolds number is used to describe the type of flow (for calculations of Reynolds number, see Appendix A). The flow is said to be laminar when Reynolds number is below 2000, and preferably below 20. Any roughness or sharp edges in the pipes or flow cell can cause local turbulence [13].

Two or more laminar flows that are brought together in a narrow channel will flow in parallel without turbulence and the only mechanism of mixing is through diffusion across the interface. With a small flow cell volume (<100 nl) and moderate flow rates (<100 µl/min), the flow is non-turbulent and the mixing of liquids between the lanes is negligible [12].

For the Y-flow cell, having two inlets, the position of the liquid interface can be approximated by the expression[4]:

[4] Requires a thin layer flow cell, i.e. w>> h where w is the widht and h is the height of the flow cell

$$Liquid\ Interface = w\frac{Flow\,rate1}{Total\,flow\,rate}$$

where the *Total flow rate* is the sum of all flow rates (Flow rate1 + Flow rate2) and w is the width of the flow cell [8].

In the case of three inlets, as in the PSI-flow cell, there will be two interfaces and both the position and width of the middle flow (sample flow) can be selected by varying the two buffer flow rates and the sample flow rate. The position of the interfaces is approximately determined by the following equations:

$$Liquid\ Interface1 = w\frac{Flow\,rate1}{Total\ flow\,rate}$$

$$Liquid\ Interface\,2 = w\frac{Flow\,rate1 + Sample\ flow\,rate}{Total\ flow\,rate}$$

where Total flow rate = Flow rate1 + Flow rate2 + Sample flow rate, and w is the width of the PSI-flow cell [8].

The above expressions are however only approximations of the position of the liquid interface. The velocity of the flow is shaped as a parable with close to zero velocity near the flow cell walls and maximum velocity found in the middle. The above expressions do not compensate for this so-called velocity profile.

Because the linear flow rate is lower near the walls of the flow cell, a larger area is needed to give the same volume flow rate near the walls as in the middle and the interface will be moved accordingly. A small change of the buffer flow rate will result in a larger displacement of the interface when it is close to the walls than if it is in the middle [8].

2.4.2 Improved signal quality (and resolution of fast kinetics) with HA

With hydrodynamic addressing the reference spot and detection spot can be contained within the same flow cell. This results in an improved referencing as it minimises the time lag that arises in serial flow cell configuration due to the physical separation of the flow cells. Signal noise caused by temperature variations between the reference and detection spot and mechanical disturbances are eliminated leading to increased precision in the measurements. Another problem avoided with HA is the higher dispersion seen in flow cells further downstream with the serial configuration [12].

2.5 INJECTION TECHNIQUES FOR FAST KINETICS

2.5.1 Lane shift

In the PSI flow cell it is possible to direct the sample flow to different lanes on the sensor surface by the principle of hydrodynamic addressing [8]. The width of the

sample lane can also be selected by adjusting the relative flow rates. The sample is introduced in the flow cell before the injection start. The buffer flow rates and sample flow rate are adjusted to position the sample lane dear of the detection spot and to achieve the desired width of the sample lane (preferably covering two detector spots, one for measuring and one reference spot). At the injection start, buffer flow 1 is increased and buffer flow 2 decreased pushing the sample lane to the detection and reference spot (figure 6). At the end of the injection, the previous buffer flow rates are restored to move the sample lane away from detection area. The sample flow is kept constant during the whole injection. This sample injection method is called lane shift. In the lane shift method, the dead volume from valve to flow cell is eliminated and the rise and fall times are only limited by the time it takes to move the interface from one position to the other. The switch between buffer and sample will be rapid and efficient since the volume needed to move the interface is much smaller than the volume needed to fill the whole flow cell.

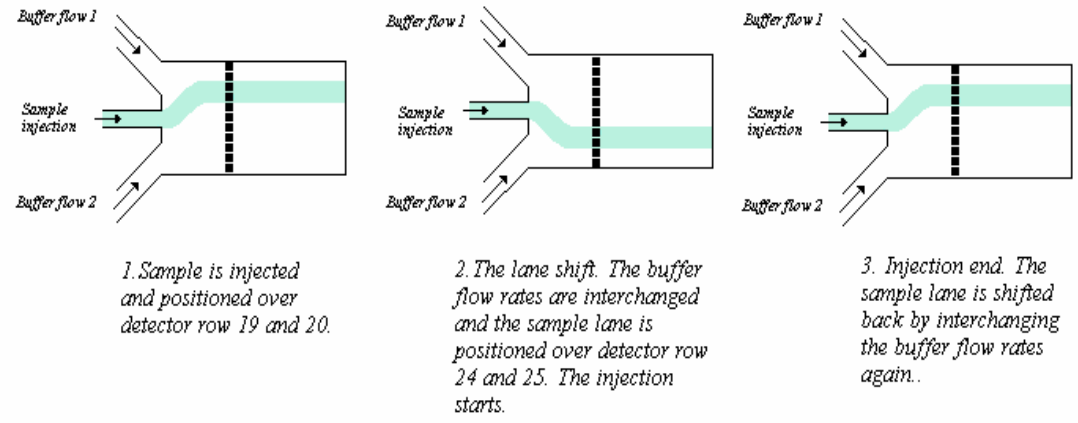

Figure 6. Schematic illustration of the lane shift in the PSI-cell.

2.5.2 Stealth inject

In the Y-cell the liquid exchange rate can be improved by the stealth inject technique. The sample inlet and a narrow lane along one flow cell wall are primed with sample by initiating a low sample flow rate just prior to sample injection (figure 7). With a sample flow rate much lower than the buffer flow rate, the primed part is kept outside the detection area. At the start of the injection, the buffer flow is stopped and the sample rate is increased and the flow cell is filled with sample. The time when dispersion can occur is decreased to the time is takes to fill the flow cell since the dead volume between the valve and the flow cell is reduced to zero. Decreased dispersion results in faster liquid exchange in the flow cell (shorter rise and fall times), and hence increased resolution of fast interactions. At the end of the injection, the reversed process may be used for a fast exchange of sample to buffer.

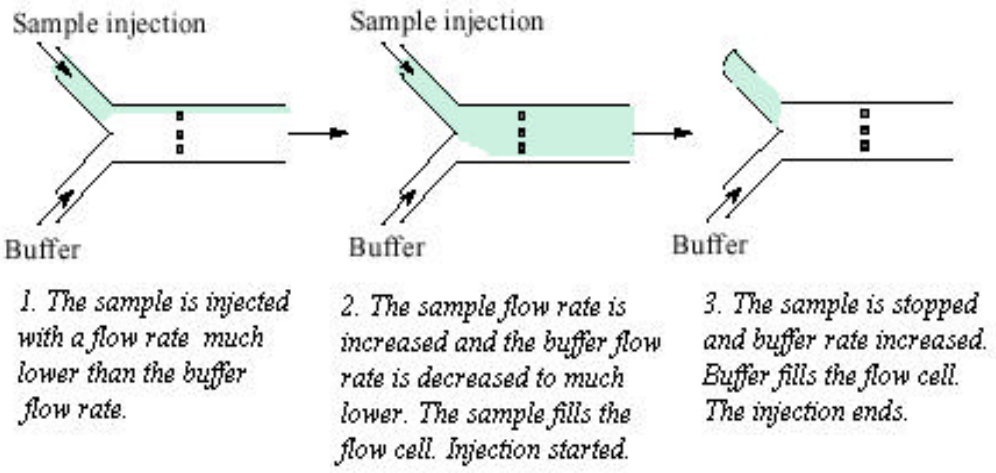

Figure 7 Schematic illustration of the stealth inject.

3 MATERIALS AND METHODS

3.1 INSTRUMENTATION AND SOFTWARE

The sensor chips used were CM-5 surfaces (Carboxymethylated dextran matrix, Biacore AB, Uppsala, Sweden). Rise and fall times were measured using a Biacore 3000, a Biacore S51 prototype and a Biacore 3D-PSI prototype. Data was presented as sensorgrams by the BIACORE 3000/ S51 control software and evaluated using the BIAevaluation (BIAeval) software, version 3.0 (Biacore AB, Uppsala, Sweden).

Injection methods were written in the Method Definition Language (MDL) in the Biacore control software. For the kinetic analysis in Biacore S51 prototype, the application wizard for compound characterisation was used, and Biacore S51 Evaluation software and BIAeval was used to evaluate the data from both the 3D-PSI and S51 prototype.

3.2 MODIFICATIONS OF S51 PROTOTYPE TO PROTOTYPE 3D-PSI

The prototype 3D-PSI used was a modified Biacore S51 prototype. A new mould was used to make the 3D-PSI flow cell. The IFC used were also modified, unnecessary valves were blocked and new channels with millimetre precision were made with surgical operations. Because of the extra inlet, an extra buffer pump was added and the connector block was modified to fit the extra tubing from the second buffer pump. To connect the second pump the electronics had also been modified. New valve commands were added in the software (Appendix B) and these were used in the new injection methods as well as in washing, prime and stand-by.

3.3 RISE AND FALL TIMES MEASUREMENTS

HBS-N (Aqueous buffer containing 0.01 M HEPES pH 7.4, 0.15 M NaCl; Biacore AB, Uppsala, Sweden) was used as running buffer in Biacore S51 and Biacore prototype 3D-PSI while HBS-EP (As HBS-N, with 3 mM EDTA and 0.005 % (v/v) Surfactant P20) was used in BIACORE 3000. A ~1 % glycerol solution (~1200 RU response) was used in all rise and fall time measurements, unless stated otherwise. Measurements were made at 25°C.

3.3.1 Detection spots

The detection spots in the flow cells correspond to different detector rows. In Biacore S51 there are three detection spots, spot 1, reference spot (r) and spot 2. They correspond to detector rows 17, 19 and 21 respectively. In the Y-cell there are seven detector rows numbered from 16 to 22, where 16 and 22 are adjacent to the flow cell walls of flow cell 1. With the present optical system, there are 11 detector rows for the PSI-cell. They are numbered from 17 to 27, where 17 and 27 are at the flow cell walls and 22 in the middle.

3.3.2 Normal inject in Biacore 3000 and Biacore S51 prototype

The rise and fall times for a regular injection were measured in BIACORE 3000 and Biacore S51 prototype. The sample flow rates were 5 µl/min, 10 µl/min, 30 µl/min and 90 µl/min, and preceding each new flow rate, three buffer start-up cycles were run to avoid temperature fluctuations. BIACORE 3000 was run in serial-channel mode and in Biacore S51 all three spots were used in one of the flow cells and the kin_x command was used for the injection.

The rise and fall times with the normal inject in Biacore S51 were measured at 40 Hz with sample flow rates 5, 10, 30, 60 and 270 µl/min. The standard deviation for each flow rate was calculated, and the average rise and fall times plotted against the flow rate. The rise and fall volumes were also calculated and plotted using Excel.

3.3.3 Lane shift

In the 3D-PSI prototype rise and fall times measurements were made using the lane shift injection method. Several combinations of buffer flow rates and sample flow rates were tested to study the positioning of the liquid interface, the pulse appearance, the width of the sample lane, noise level and baseline stability. The sample flow rate was varied from 5 µl/min to 90 µl/min, and the total flow rate was varied between 60 µl/min and 200 µl/min. The addition of three air-segments separating the sample from buffer was tried in order to reduce the drift seen in the pulse response. Discarding 0 µl or 30 µl of the sample before the injection was also compared to study the effect on the curvature of the pulse.

In order to allow for reference subtraction, the sample lane has to cover at least two detector rows completely. The liquid interface has to be positioned so as to leave both these detector rows undisturbed with a stable baseline before the injection and with a 100 % pulse response level. The buffer flow rates and the total flow rate were adjusted to meet these requirements for a given sample flow rate. The sample lane were positioned to cover spot 19 and 20 before the injection start, and at the start of

the injection symmetrically shifted to spot 24 and 25. The total flow rate was varied to have the sample flow rate equal 25 % or 30 % of the total flow rate. The sample lane width was hereby varied and the noise and coverage of the detector rows studied. The resulting rise and fall times were compared.

The sample flow rates used for rise and fall times measurements were 5, 10, 30, 60, 90 and 270 µl/min. The time resolution was 10, 20 or 40 Hz, depending on the accuracy and number of detector rows needed. At 20 Hz the two possible settings of ad_scans and exp_time were compared. Measurements of rise and fall times at a changed sample flow rate were always preceded by five buffer start-up cycles to avoid temperature fluctuations. Ten sample injections at flow rates 5, 10, 30, 60, 90, 270 µl/min and 40 Hz resolution were used to calculate the average and standard deviation of the rise and fall time for each flow rate. The average rise and fall volumes were also calculated.

3.3.4 Stealth inject

Normally the detector rows corresponding to spot 1, 2 and the reference spot are used, but to be able to study the position of the liquid interface the settings were changed to allow for detection of the whole flow cell, using all detector rows. The low sample flow rate, referred to as the priming flow, used during the so-called priming of the flow cell, was varied between 1 µl/min and 16 µl/min with a buffer flow rate of 30 µl/min to study the position of the liquid interface during the priming. To avoid temperature fluctuations the buffer flow rate and the injection sample flow rate were set to equal each other. The liquid interface was then positioned on detector row 16 and 17, and the rise times at flow rates 5, 10, 30, 60 and 90 µl/min for the two positions were compared. Measurements were done with 10 Hz time resolution.

The process of priming the flow cell with a low flow rate was reversed for the cut down, but with the buffer left running with a low flow rate during the sample injection. The fall times were measured for flow rates 30 µl/min and 60 µl/min and compared to the fall times for normal cut down. The rise times were measured ten times with 40 Hz time resolution for sample flow rates 5, 10, 30, 60 and 90 µl/min. Average and standard deviation was calculated and plotted against flow rates.

3.3.5 Rise and fall times for samples with different diffusion constants

The rise and fall times for samples with different diffusion constants were measured in Biacore S51 prototype. The samples were albumin, glycerol and sucrose, listed below, all diluted in HBS-N running buffer to give a response level of about 1000 RU. The normal injection method in Biacore S51 with 40 Hz time resolution and flow rate 10 µl/min was used. Following five start-up cycles with buffer, each sample was run 5 times.

Table 1 Diffusion coefficients and molecular weight of the different samples.

Sample	Diffusion coefficient (m^2/s)	Molecular weight
Human Serum Albumin (5 mg/ml)	6.15E-11	64000
Sucrose	5.20E-10	337
Glycerol (1%)	1.06E-9	92

3.3.6 Rise and fall time determination

Analyses of rise and fall times were done using the BIAevaluation software, version 3.0 (Biacore AB, Uppsala, Sweden). The rise time was defined as the time taken for the pulse to go from 1 % response to 99 % response and the opposite for the fall time. Using BIAevaluation, the sensorgrams were first normalised separately. In cases where the pulse level was unstable with a drifting response, this was taken into consideration during the normalisation by only selecting the relevant area. When analysing the 10-replicas, the curves were normalised together unless the difference between the pulse responses was pronounced.

Following normalisation, a curve alignment was done to set the injection start of all curves to the time step just before exceeding 1 % response. The rise time was then read out as the time when 99 % level was reached. When measuring fall times, the injection end was set to the time just before decreasing below 99 % response, and the fall time was read out as the time when the signal fell down to 1 %. All steps were performed manually, and the times were read out as the time intersecting the 99 % respectively 1 % level by zooming in on the sensorgrams.

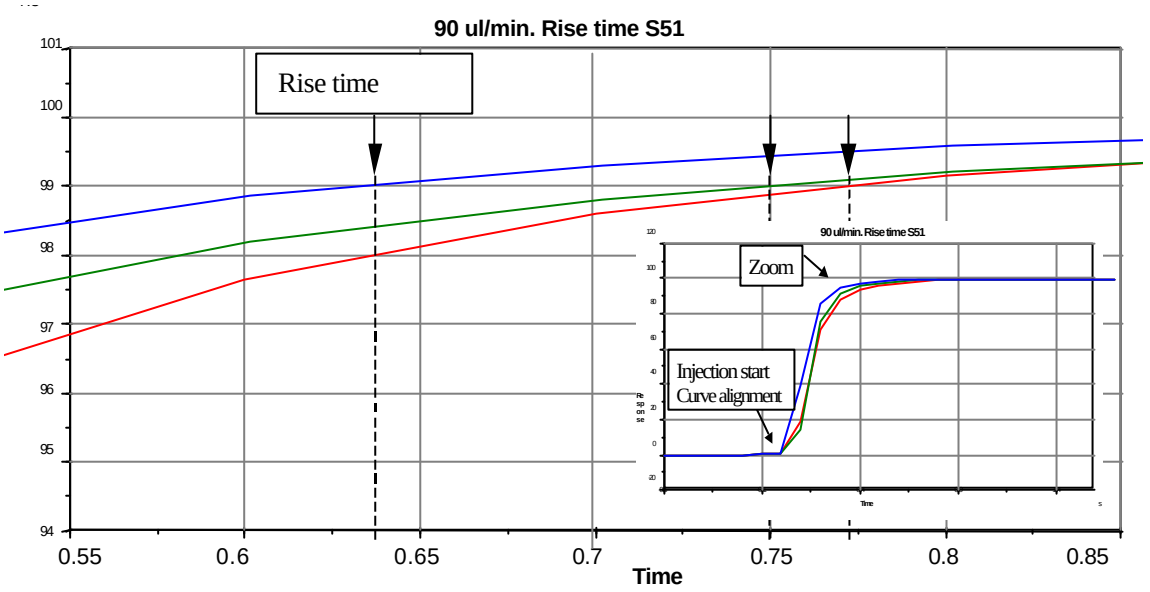

Figure 8 Illustration of rise and fall time measurements.

3.4 INCREASED TIME RESOLUTION

By increasing the sampling rate the time resolution was increased. To be able to use higher data collection rates than 10 Hz, a number of parameters had to be changed. First, the minimum allowed value of the "MODE –d" option under [CURVE:SWEEP_ST] was changed in CMD.INI, and a new file was created called Bme2Srv.INI (from disc) to support data collection rates higher than 10 Hz. Normally it takes 760 µs to read the whole detector. Ad_exptime represents the time each pixel is exposed before they are read off, it can be changed by a factor 1,2,4,8 or 16 and the exposure time is prolonged by this factor. Ad_scans is how many times the detector is read off and averaged for one output data. During one sample period, there must be enough time to complete the averaging and therefore,
$760e^{-6} * ad\_exptime * ad\_scans$ must be shorter than the sample period, i.e.

ad_exptime∗ad_scans∗sampling_rate<1/760e^{-6} (=1280 for 10 Hz). For runs with increased sampling rate, the default values of these parameters were therefore changed according to table 2.

Table 2 Settings changed for increased time resolution. Settings for 10 Hz unchanged for sampling rates lower than 10 Hz.

Sampling rate (Hz)	Sample period (s)	Intensity	Ad_exptime	Ad_scans	Number of detector rows
10	0.1	0.75	2	64	11
20	0.05	0.75	2	32	3 (6)
		1.0	1	64	
40	0.025	1.0	1	32	1 (3)

The intensity of the light was increased to compensate for shorter exposure times, and the ad_cut_limit was decreased. When the sampling rate is increased the number of detector rows that can be used will be limited to avoid problems with data transfer between the instrument and the computer [14].

3.5 IMMOBILIZATION OF HSA

3.5.1 Biacore S51 prototype

Human serum albumin (HSA, 32µg/ml in 10mM sodium acetate pH 5.0) was immobilized using the immobilization wizard in Biacore S51 control software. A standard amine coupling method was used for the immobilization [10]. EDC/NHS was injected for 7 min to activate the surface and ethanolamine 7 min for the deactivation. HSA was injected at a flow rate of 10 µl/min, either for 1-4 min or using the option "aim for immobilized level" with 50 µM NaOH surface regeneration, to yield immobilization levels between 3000 and 6300 RU. The immobilizations were conducted at 23°C in PBS running buffer (67 mM phosphate buffer, pH 6.7).

3.5.2 PSI-cell

HSA (32µg/ml in 10mM sodium acetate pH 5.0) was immobilized using the standard amine coupling procedure at 25°C in PBS running buffer (67 mM phosphate buffer, pH 6.7). Detector rows 24 and 25 were used as reference spot and measuring spot, respectively. EDC/NHS was mixed 1:1 prior to injection and injected for 7 min. Following surface activation, HSA was injected at a flow rate of 13 µl/min for 4 min. Buffer flow rates were adjusted to position the ligand flow covering all of detector row 25, but as little as possible of the reference row 24. Deactivation was done injecting ethanolamine over the whole surface for 7 min at 25 µl/min with buffer flow rates set to zero. Typical immobilization levels ranged from 3000 to 7000 RU, with less than 1 % signal from reference spot.

3.6 KINETIC DETERMINATION OF LOW-MOLECULAR DRUGS INTERACTING WITH HSA

5 mM (Warfarin, Digitoxin) and 50 mM (Naproxen, Phenylbutazone) stock solution of analytes in 100 % DMSO were carefully diluted in running buffer (PBS with 5 % DMSO) to analyte concentrations ranging from 0 to 50 µM and a final DMSO concentration of 5%. Instead of using solvent correction to correct for large bulk effects, variations in DMSO concentration was minimised by careful dilution of the sample. Each time, 5.0 µl of the sample (100 % DMSO) was aspirated using the same pipette and added to 95 µl PBS buffer, and then diluted in running buffer to the desired concentration. The running buffer was prepared fresh before each run and the DMSO volume added weighed. By this procedure and by choosing a rather low immobilization level, the resulting bulk effects were sufficiently low (<30 RU) to leave out solvent correction. Zero concentration samples was always included and prepared using the same procedure.

Kinetic runs were performed in parallel on the S51 and 3D-PSI prototype, with 3-5 buffer start-up cycles and with a sample flow rate of 30 µl/min. In 3D-PSI the lane shifts was used and in Biacore S51 the normal inject, each sample concentration was injected in duplicates. Analyses were performed at 23/25 °C. The reference and zero-concentration responses were subtracted (double referencing) in BIAeval before analysing the sensorgrams.

4 RESULTS

4.1 LANE SHIFT IN 3D-PSI

4.1.1 Flow rates, lane width and noise level

The higher sample flow rates and a low total flow rate gave the lowest noise levels. A too high sample flow rate compared to the total flow rate resulted in a too wide sample lane covering most of the detector rows unsuitable for the lane shift. A sample flow rate of 25-30 % of the total flow rate gave a reasonable lane width with a low noise level. The comparison of 25 % and 30 % sample flow rate showed no relevant difference in rise and fall times but less noise and a better positioning was achieved with the wider sample lane (30%). The flow was laminar with a Reynolds number <20 in the flow cell for all flow rates used.

High sample flow rates gave an s-formed pulse response. The addition of three air-segments did not correct for this curvature of the pulse. The curvature was avoided when discarding of 30 µl of the sample before the injection and a square wave like pulse was obtained. The rise and fall times were however unchanged as compared to when 0 µl was discarded.

By choosing a symmetric lane shift, the lane shift was accomplished simply by interchanging the two buffer flow rates. Detector rows 19,20 and 24,25 were used for

the shift. To position the sample lane over detector row 19 and 20, buffer flow 1 and 2 were 12 µl /min and 58 µl/min respectively for a sample flow rate of 30 µl/min. For the shift, the buffer flow rates were interchanged and the sample flow rate constant.

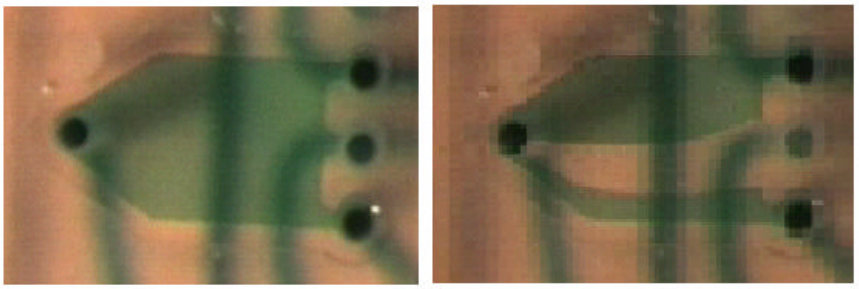

Figure 9 Picture of the PSI cell performing a lane shift. The running buffer was coloured green for visualisation. To the left is a picture of the PSI cell with only buffer flow running. To the right is a picture of the PSI cell showing the sample lane, taken at a flow rate of 60 µl/min. Flow channels are seen in the background.

Blank injections with buffer gave a noise level of 0.3 RU at 10 Hz. The motion of the fluid or mechanical disturbances did not give any considerable noise. Rise and fall time measurements at 20 Hz showed no difference between the two possible combinations of ad_scans and ad_exptime. Using three detector-rows instead of one in measurements at 40 Hz worked and it was checked that the instrument time corresponded to the actual time. The noise level increased with higher sampling rate, but was within acceptable levels.

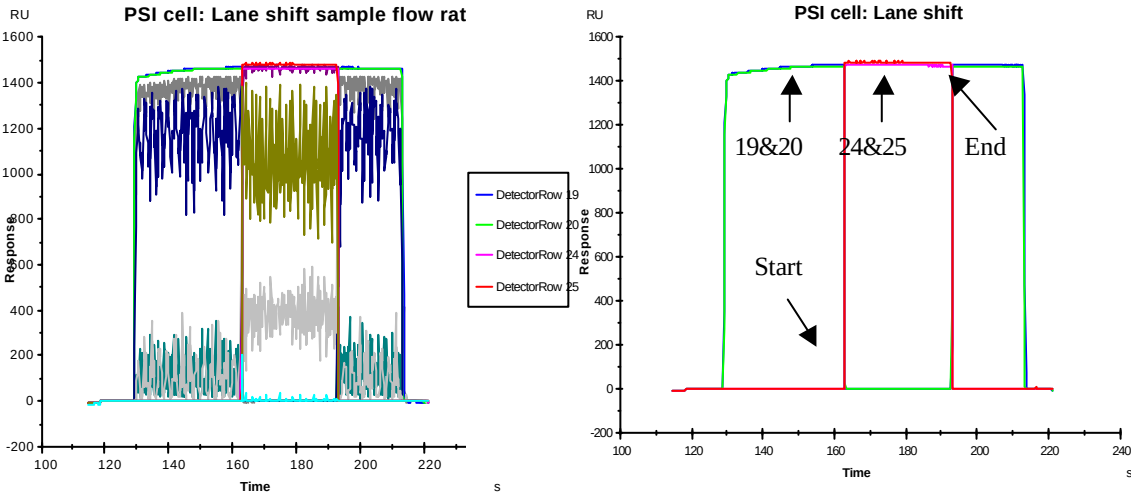

Figure 10 Sensorgram showing the lane shift in PSI. The sensorgram to the left shows all detector rows. The liquid interface is positioned over the detector rows with large noise levels, and with a response level between zero concentration and hundred percent concentration. To the right, only the detector rows used in the shift are seen. Before the injection start, the sample lane is positioned over detector row 19 and 20, having full response. At the injection start, detector rows 24 and 25 rises from zero concentration to maximum response. The baseline is undisturbed before and after the injection.

4.1.2 Rise and fall times with the lane shift

Average rise and fall times measured at 40 Hz for different flow rates are shown in table 3. Average rise and fall times and volumes are plotted against flow rate in figure 11 and 12, with error bars representing the standard deviation. The rise time decreases with increasing flow rate and the rise volume increase linearly with the flow rate. A small difference in rise and fall times between the detector rows is seen, for the rise time, detector row 24 is on average 0.02 seconds faster. A larger standard deviation is seen for the rise volume at a flow rate of 270 µl/min.

The fall times are also improved when increasing the flow rate. The fall times are about the same size as the rise times for different flow rates with the exception of 5 µl/min where the fall times are about half as long as the rise times. As for the rise volumes, the fall volumes increased with increasing flow rates (figure 12). The largest improvement is obtained for low flow rates, and increasing the flow rate above 60 µl/min does not give any considerable improvement in neither the rise nor fall time.

Rise times PSI	Flow (ul/min)	**5**	**10**	**30**	**60**	**90**	**270**
Spot r/24 (s)	Average:	0,59	0,25	0,15	0,11	0,08	0,06
Spot 25 (s)	Average:	0,61	0,31	0,16	0,12	0,10	0,08
Fall times PSI							
Spot r/24 (s)	Average:	0,33	0,21	0,12	0,09	0,08	0,06
Spot 25 (s)	Average:	0,33	0,21	0,11	0,09	0,08	0,11

Table 3 Average rise and fall times for different sample flow rates for the lane shift in PSI. Measurements at 40 Hz in 10-replicats. For all values, see appendix C.

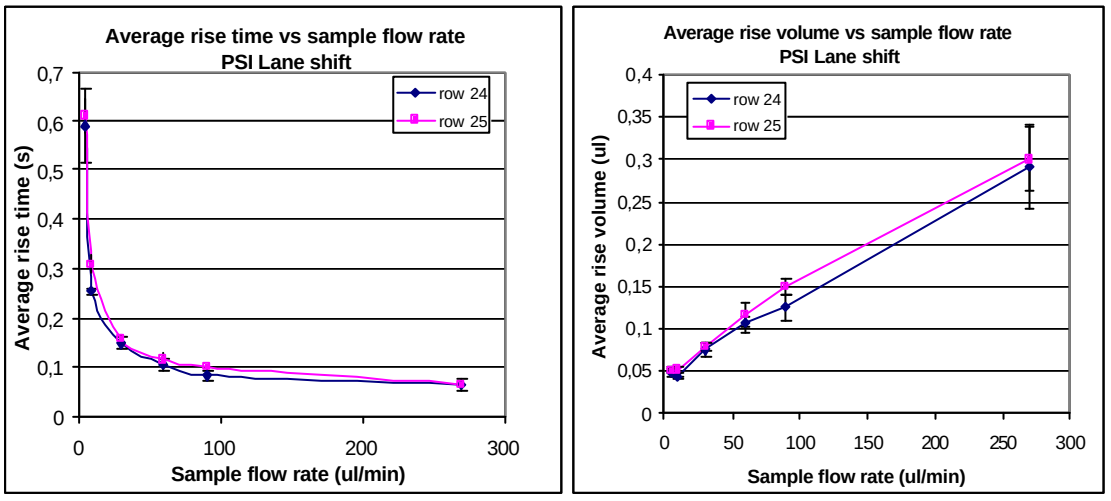

Figure 11 Plot of the rise time vs. flow rate and rise volume vs. flow rate for lane shift in PSI. Standard deviation represented by error bars. One measurement at flow rate 270 µl/min was not included in average and standard deviation calculation as the curve was disturbed.

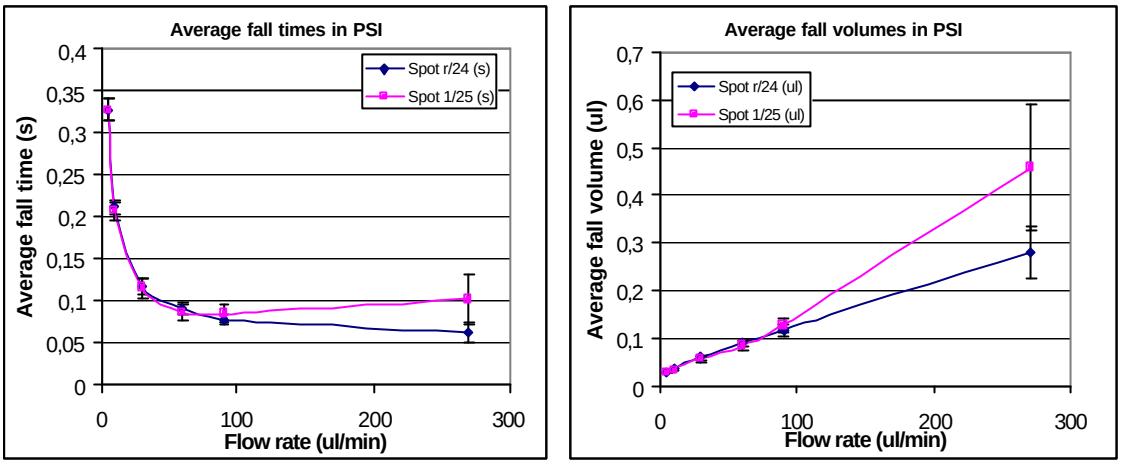

Figure 12 Plot of the fall time vs. flow rate and fall volume vs. flow rate for the lane shift in PSI. Standard deviation represented by error bars. Average of ten injections, one measurement at 270 µl/min was not included as the curve was disturbed.

4.2 STEALTH INJECT IN BIACORE S51

The rise time is shorter when the liquid interface is positioned on detector row 17 instead of detector row 16. The positioning over detector row 16, which is the detector row closest to the flow cell wall, gave a more prominent curvature of the pulse and did not work for low flow rates (<10 µl/min). Hence, the measurements were made positioning the liquid interface on detector row 17 (spot 1). Detector row 18, 19 and 20 was used for rise and fall times measurements. The baseline was stable and although the linear flow rate was changed, no temperature fluctuations were seen when the sample was let in.

Reversing the procedure during the so-called cut-down worked but resulted in slightly increased or unchanged fall times and hence no further measurements were made. The average rise times and rise volumes for different flow rates are shown in figure 13 and table 4. The rise time is shorter the closer the detector row is to the liquid interface, and the shorter rise times are seen for higher flow rates. For the flow rate 30 µl/min a minima in the rise volume is seen. With the stealth inject, the rise times are improved with on average a factor six compared with the normal inject.

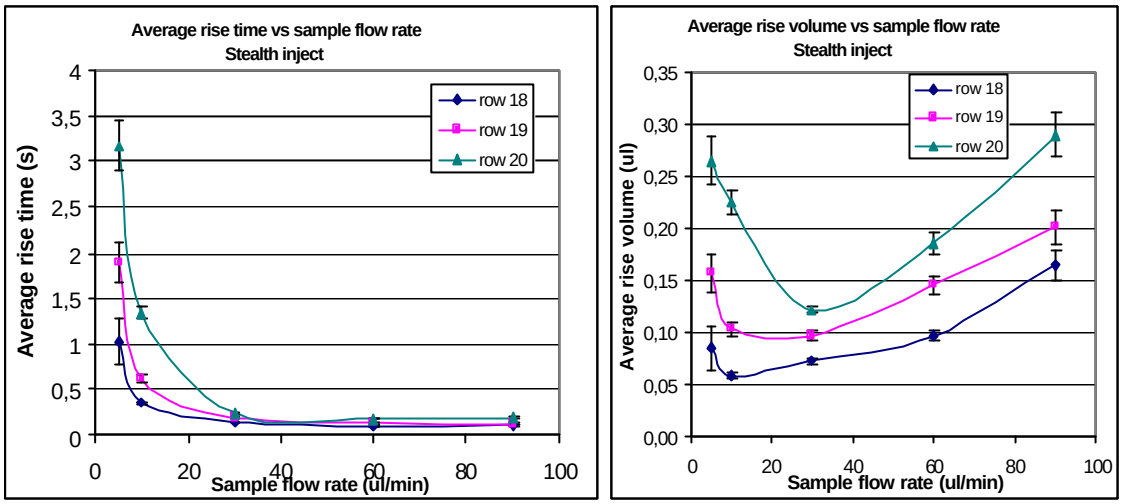

Figure 13 Average rise times and rise volumes plotted against flow rates for the stealth inject in the Y-cell. Standard deviation represented with error bars. Measurements at 40 Hz, 10 replicas.

Table 4 Average rise times and rise volumes with the stealth inject measured at 40 Hz.

Average rise time (s)		Sample flow rate(ul/min)			
Detector row	5	10	30	60	90
18	1,02	0,35	0,14	0,10	0,11
19	1,89	0,62	0,19	0,15	0,13
20	3,17	1,35	0,24	0,19	0,19
Average rise volume (ul)		Sample flow rate (ul/min)			
Detector row	5	10	30	60	90
18	0,09	0,06	0,07	0,10	0,16
19	0,16	0,10	0,10	0,15	0,20
20	0,26	0,22	0,12	0,19	0,29

4.3 COMPARISON OF THE RISE AND FALL TIMES

4.3.1 Normal inject in Biacore 3000 and Biacore S51

Table 5 shows the rise and fall times measured at 10 Hz in Biacore 3000, Biacore S51 prototype and prototype 3D-PSI. In Biacore 3000 the rise time and fall time increases for flow cells that are further downstream. A difference between the detection spots in the Y-cell in Biacore S51 can also be seen. The longest rise time is measured for spot 2, which also is the spot that is the furthest away from the sample inlet. During the cut-down, spot 1 is furthest away from the buffer inlet and has as seen in table 5 also the longest fall times. The fall times in Biacore S51 are about one tenth of the fall times in Biacore 3000. This is largely due to the use of two inlets with one inlet used separately for buffer.

Table 5 Comparison of rise and fall times for different flow rates measured in Biacore 3000, Biacore S51 prototype and prototype 3D-PSI. The calculated rise and fall volumes are also shown. Measurements at 10 Hz.

RISE TIMES /VOLUMES		BIACORE 3000				Biacore S51			PSI	
Flow rate	Flow cell/spot	1	2	3	4	1	r	2	24	25
5 ul/min	Rise time (s)	7,6	14,1	15,6	19,9	10,2	13,4	17,6	0,5	0,8
	Rise volume (ul)	0,63	1,18	1,30	1,66	0,85	1,12	1,47	0,04	0,07
10 ul/min	Rise time (s)	3,5	8,0	8,6	11,0	4,7	5,8	9,7	0,4	0,5
	Rise volume (ul)	0,58	1,33	1,43	1,83	0,78	0,97	1,62	0,06	0,08
30 ul/min	Rise time (s)	1,4	3,3	3,6	4,6	1,8	1,5	2,2	0,3	0,3
	Rise volume (ul)	0,71	1,65	1,80	2,31	0,88	0,76	1,11	0,14	0,15
90 ul/min	Rise time (s)	0,7	1,6	1,8	2,1	0,8	0,7	0,7	0,3	0,3
	Rise volume (ul)	1,05	2,34	2,64	3,12	1,16	0,99	1,08	0,42	0,44

FALL TIMES / VOLUMES		BIACORE 3000				Biacore S51			PSI	
Flow rate	Flow cell/spot	1	2	3	4	1	r	2	24	25
5 ul/min	Fall time (s)	5,2	13,0	14,7	19,3	1,6	1,0	1,4	0,5	0,4
	Fall volume (ul)	0,43	1,08	1,23	1,61	0,13	0,09	0,11	0,04	0,03
10 ul/min	Fall time (s)	2,6	7,3	8,1	10,7	0,6	0,4	0,5	0,4	0,3
	Fall volume (ul)	0,43	1,21	1,34	1,78	0,09	0,07	0,08	0,06	0,05
30 ul/min	Fall time (s)	1,1	2,7	3,2	4,1	0,4	0,3	0,3	0,2	0,2
	Fall volume (ul)	0,53	1,33	1,58	2,05	0,19	0,15	0,15	0,12	0,10
90 ul/min	Fall time (s)	0,8	1,2	1,6	2,0	0,3	0,3	0,3	0,2	0,2
	Fall volume (ul)	1,17	1,80	2,36	2,97	0,44	0,39	0,38	0,30	0,29

The average rise and fall times and volumes for the normal inject measured at 40 Hz is shown in figure 14 and 15. It is seen that for low flow rates, the rise time is shorter for spot 1 than for the reference spot, but when the flow rate is increased above 10 µl/min, this is however reversed and the rise time is shorter for the reference spot. The same pattern is however not seen for the cut-down, where the reference spot is fastest for low flow rates.

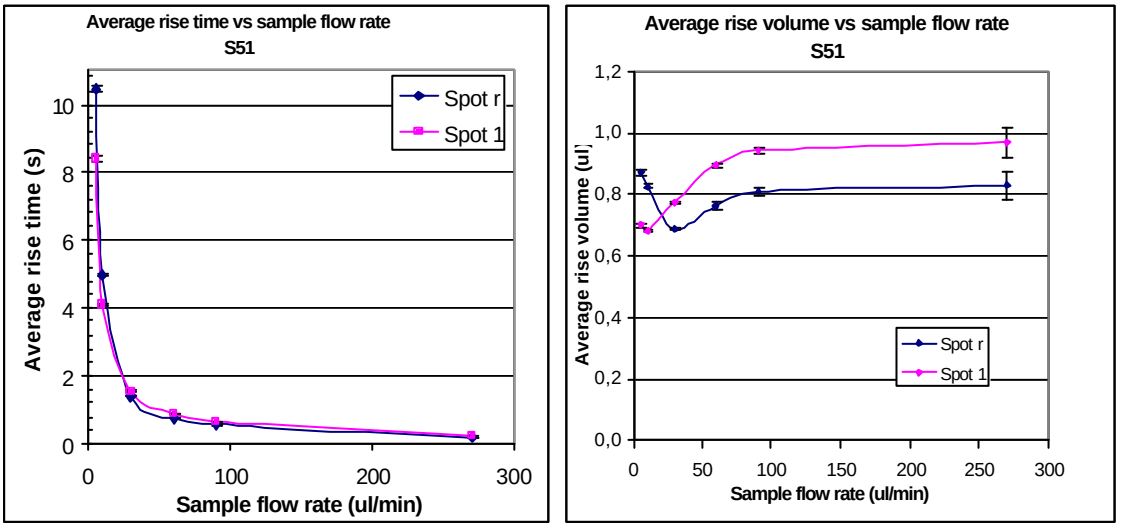

Figure 14 To the left, average rise time plotted against flow rate measured with the normal inject in Biacore S51 prototype. To the right, average rise volume plotted against flow rate. Error bars showing the standard deviation.

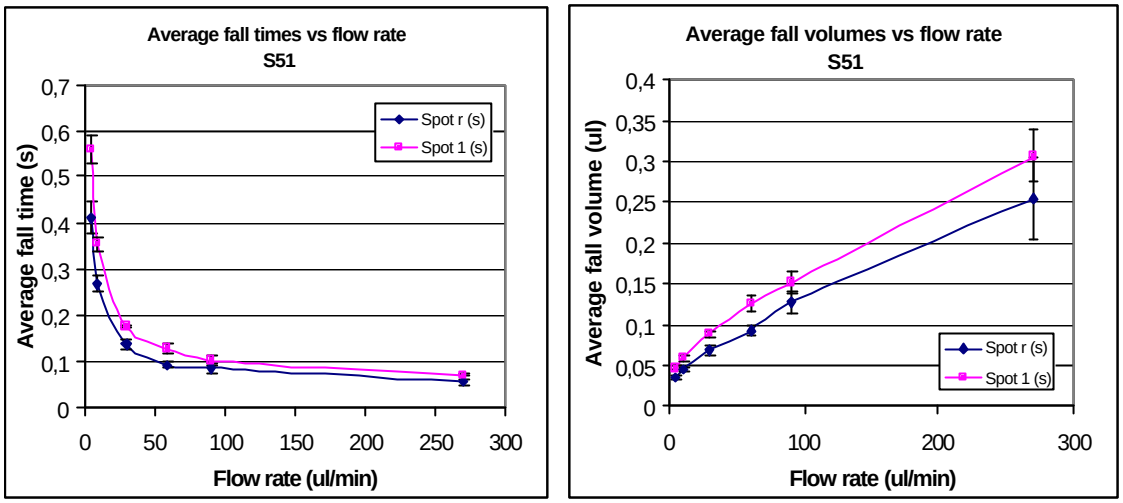

Figure 15 To the left, average fall time plotted against flow rate measured with the normal inject in Biacore S51 prototype. To the right, average fall volume plotted against flow rate. Error bars showing the standard deviation.

4.3.2 Lane shift in the PSI cell and Biacore S51

For flow rates 5-90 µl/min the rise times are on average 10 times better with the lane shift in the PSI cell than with a normal inject in Biacore S51. The relative improvement of the rise times and fall times in the PSI cell are shown in figure 16. Figure 17 compares the average rise and fall times. The greatest improvement of the rise time relative to Biacore S51 is obtained for low flow rates. The fall times are only slightly improved in the lane shift, and with the sample flow rate 270 µl/min it is even longer than with the normal inject.

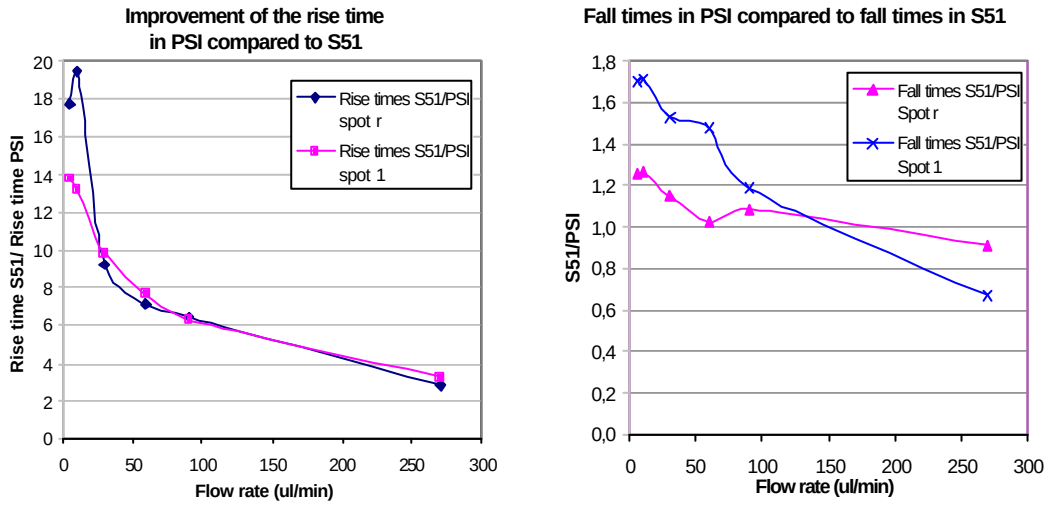

Figure 16 Comparison of the rise and fall times in S51and PSI.

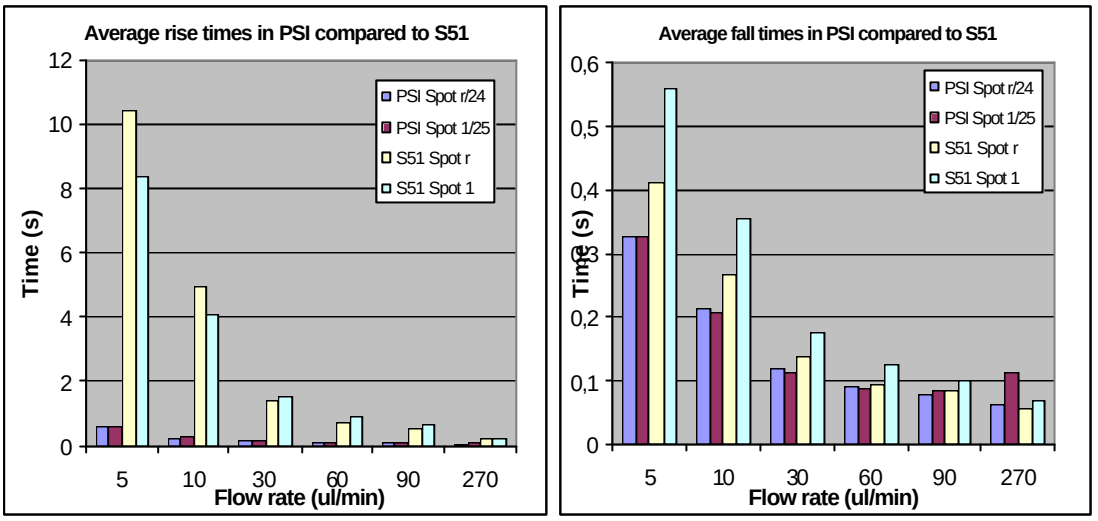

Figure 17 Comparison of the average rise times and fall times in PSI compared to S51 at different flow rates. Measurements at 40 Hz, 10 replicas.

4.3.3 Rise and fall times for samples with different diffusion coefficients

The rise and fall time for HSA was substantially larger than the average rise and fall time measured for sucrose and glycerol, as seen in figure 18.

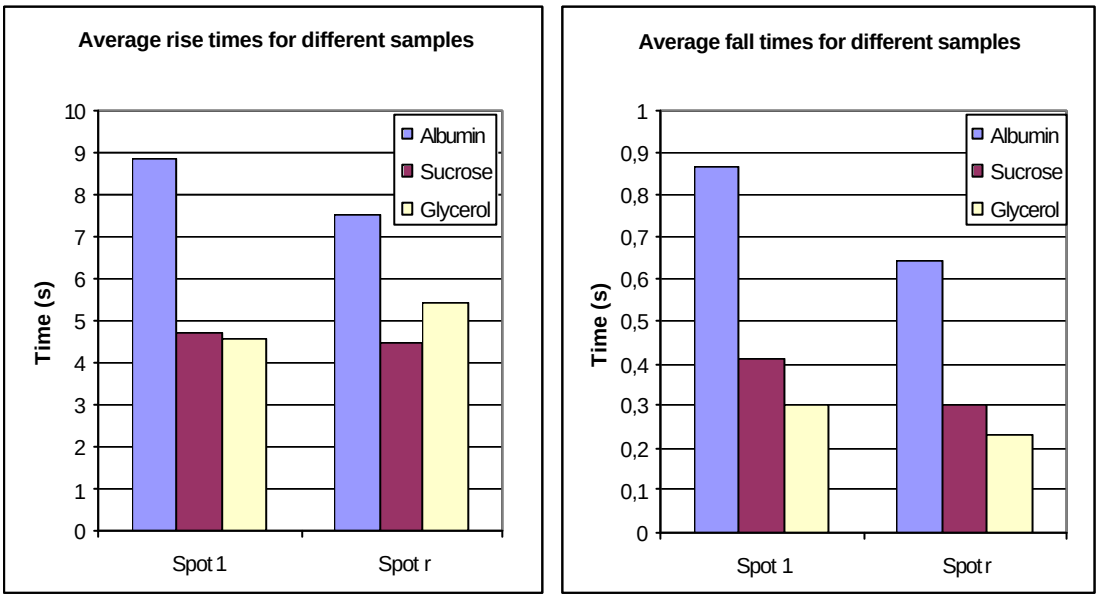

Figure 18 Average rise and fall times for different samples measured in Biacore S51 prototype at a sample flow rate of 10 µl/min. Spot 1 and reference spot shown.

A simulation of the flow profile for two analytes with different diffusion coefficients in a simplified 2D flow cell was performed in Femlab[5], as to study the effect on the rise time. The molecule with the large diffusion coefficient (glycerol) gave a less prominent velocity profile and the faster the diffusion, the shorter time to reach the surface where the measurements take place (figure 19A). With a small diffusion

[5] kindly performed by Annica Önell at Biacore AB

coefficient, as for a large molecule (here HSA) the velocity flow profile was much more pronounced and a longer time was needed for the molecules to be transported to the surface (figure 19B). The simulated rise times are approximately the same as measured rise times.

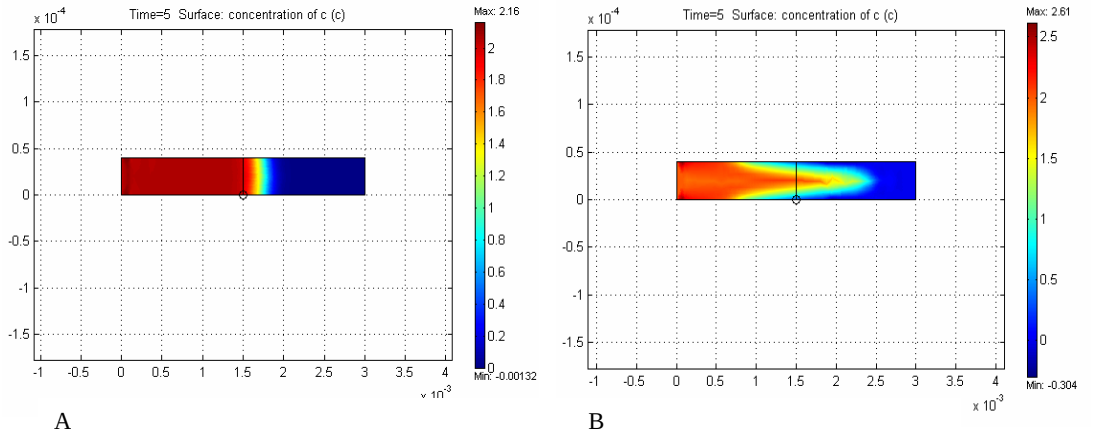

A B

Figure 19 In a) the velocity profile for diffusion coefficient $1e^{-9}$ is shown, and in b) for diffusion coefficient $1e^{-11}$. The concentration gradient in a cross section of the flow cell at time t=5 s is shown.

4.4 IMMOBILIZATION AND KINETIC DETERMINATION

The PSI-cell gave similar sensorgrams as the S51 when performing the kinetic analyses and binding curves were obtained. The bulk effects were less than 30 RU. After reference subtraction and blank subtraction, the response levels ranged from 5 RU to 50 RU. Figure 20 shows an overlay plot of the association phase of 25 µM Naproxen in S51 and PSI. The resulting binding curve from the kinetic run in the PSI cell reaches the plateau value faster than the curve from the S51 run. The noise level is higher in PSI as the measurements were made at 40 Hz compared to 10 Hz in S51.

For the concentration series, different analyte concentrations gave different response maximum, and can be used to determine the binding affinity. The sensorgrams from the concentration series in PSI were comparable with the ones from S51 (figure 21 & 22).
Although binding curves were obtained, the kinetic rate constants could not be determined. For low concentrations the association is slower but the response level is too low compared to the noise level. The association rate is still too fast to be resolved, even with the improved liquid exchange rate in the PSI-cell.

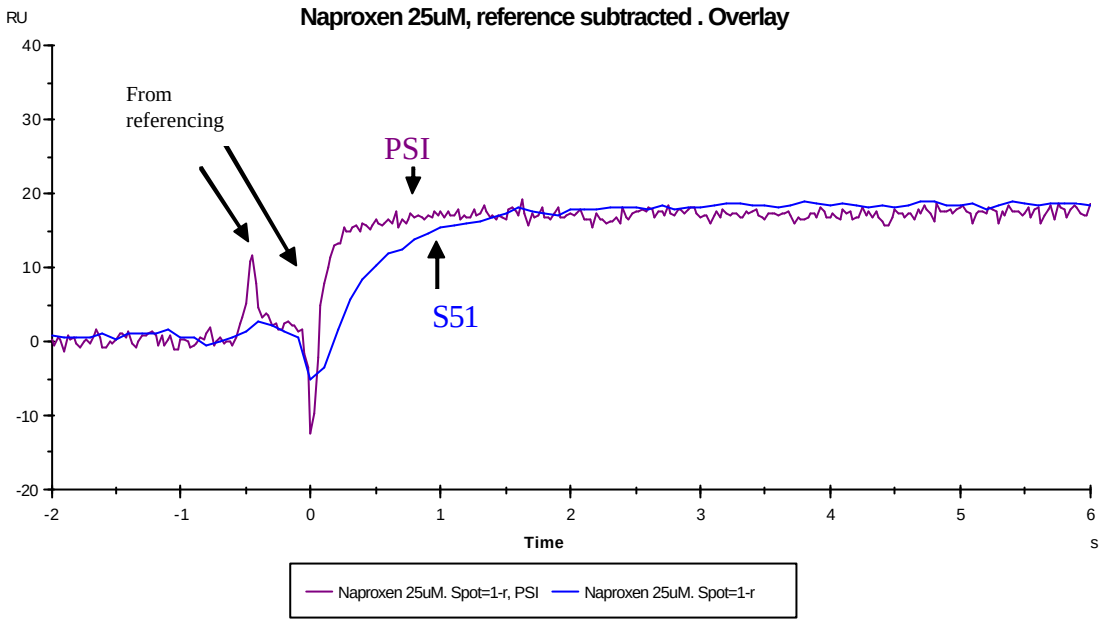

Figure 20 Overlay plot of binding curves of 25 µM Naproxen in S51 and PSI. The curves are double referenced and aligned to have the same injection start. The binding phase has been zoomed in to show the difference in rise time. The sample flow rate was 30µl/min. The higher noise level seen for PSI is due to the higher sampling rate that is used here (40 Hz compared to 10 Hz).

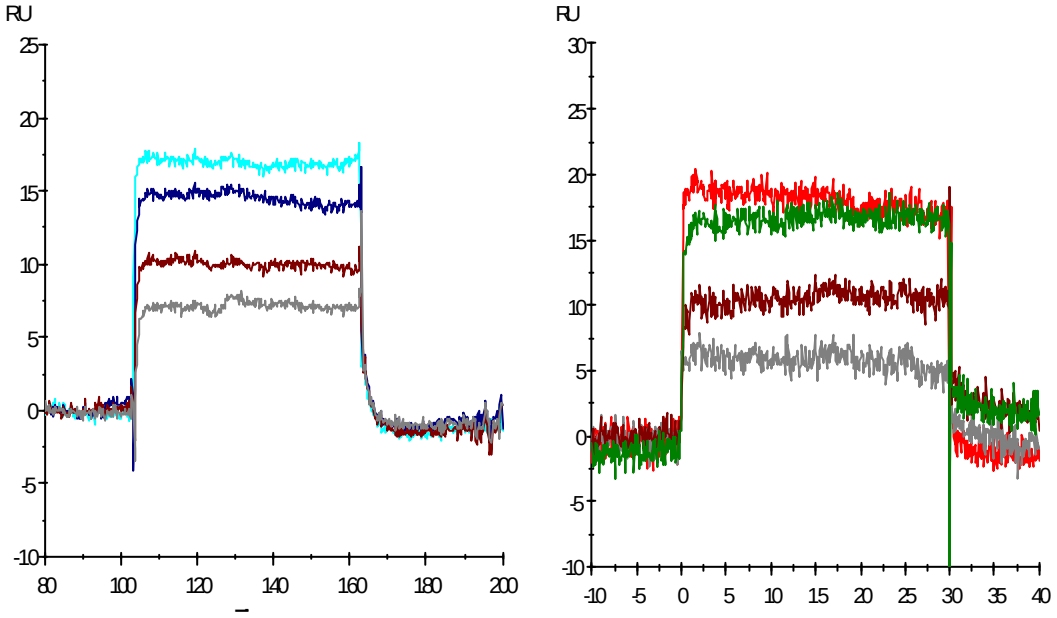

Figure 21 Concentration series (50, 25, 12.5 and 6.25µM) of Naproxen injected at 30 µl/min. The sensorgram to the left showing overlay plot of the binding curves obtained in S51 after double referencing and curve alignment. To the right, overlay plot from PSI binding data, measured at 40 Hz, which explains the higher noise level.

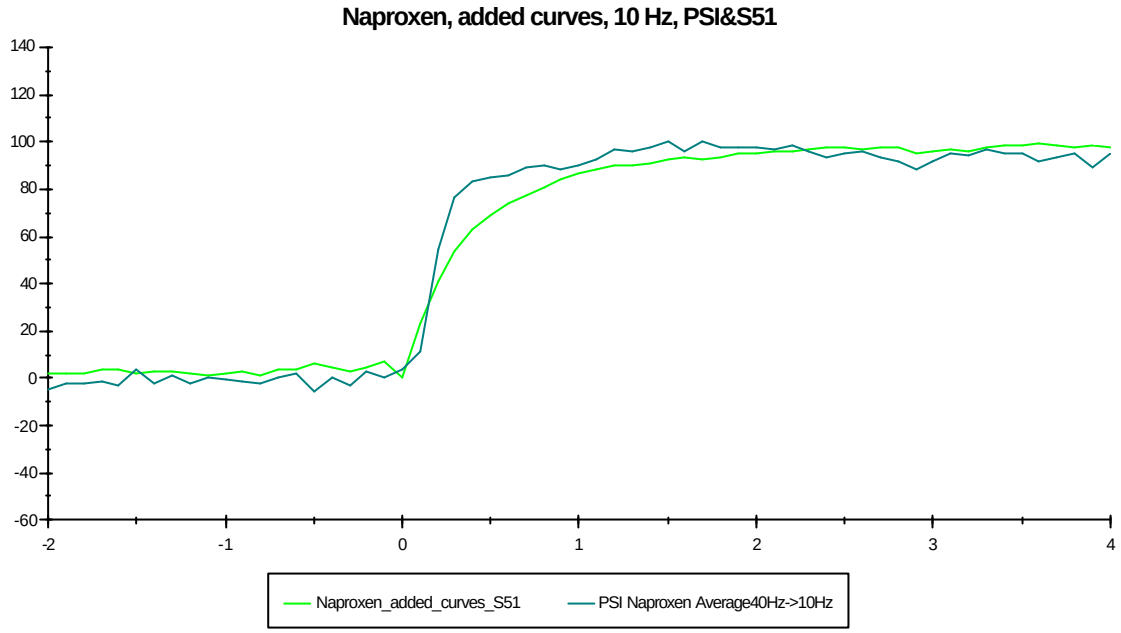

Figure 22 Overlay plot of binding curves from kinetic runs with Naproxen in Biacore S51 and prototype 3D-PSI. By averaging several curves the noise level was reduced. Both curves have been normalised and aligned.

5 DISCUSSION

5.1 UNCERTAINTY IN THE RISE AND FALL TIME MEASUREMENT

Because the determination of the rise and fall times is carried out manually there are moments where the times have the characteristics of an estimate. During normalisation of the pulse response, mechanical disturbances caused by for example valve switching or disturbances caused by differences in temperature can effect the maximum or minimum response level which in turn will effect the 1 % and 99 % level, giving different rise and fall times. With a curved pulse, it can also be difficult to determine when the drift in pulse response starts and when the rise is over. Unless having a square wave like pulse, the response was normalised separately before determining the rise and fall times, selecting an area covering only the rise or fall respectively.

Another factor effecting the accuracy of the rise and fall time measurements is the time resolution. At the 1 % level and at the 99 % level, the time is read out as the time when the curve intersects the desirable level. This time does not always corresponds to a time when the detector value was read out but will be the time the line connecting the two closest data points intersects the level of interest. With a time resolution of 10 Hz, or 0.1 second, this means that the time for the intersection lies between these two data points and can differ by ± 0.05 seconds. For both the rise and fall time, both start and end time is determined and the final time can differ by ±0.1 second. With a high flow rate the measured times are in the order of 0.1 seconds and the difference has a large effect in the final rise and fall time determination. For more

accurate data, higher sampling rate is necessary, especially for high flow rates. With 40 Hz the error in rise and fall time determination is ± 0.025 seconds, which is about 1/3 of the rise time for high flow rates.

5.2 IMPROVED RISE TIMES WITH THE PSI CELL AND WITH THE STEALTH INJECT IN THE Y-CELL

With the lane shift in the PSI cell and the stealth inject in the Y-cell the rise time was improved with on average a factor ten and six, respectively. The reduced rise time means that the liquid exchange rate from buffer to sample is faster. The faster switch between buffer and sample reduces the dispersion, as there is less time for dispersion to occur. With the lane shift and stealth inject the dead volume is avoided and the time for dispersion to occur is reduced to the time it takes to move the liquid interface across the flow cell. This contact time is only a fraction of the time it takes to fill the whole flow cell from the inlet valve. The contact time is shorter at higher flow rates giving less dispersion and faster rise times. The rise time is longer for detection spots positioned further away from the liquid interface. This could be due to the slightly longer contact time.

The dead volume is the volume from inlet valve to detection spot. In Biacore S51 this volume is 0.4 µl for the rise, and the measured rise volumes are about two times the dead volume. With the stealth inject, the measured rise times are much smaller, and the dead volume is minimised to the area in the flow cell to the detection spots, which is less than 0.035 µl. In Biacore 3000 the increased rise time for flow cells further downstream are explained by the increased dead volume and the longer time for dispersion to occur.

For the lane shift in PSI, the time delay is related to the flow rate as 1/ (flow rate)$^{1/2}$, whereas for the normal inject and the stealth inject it is inversely proportional to the flow rate. A possible explanation for this is that the flow is controlled with the pumps and not by valve operation in the PSI cell, and that the response rate of the pumps is non-linear.

Ten times faster rise times means a ten times faster buffer to sample liquid exchange rate. This improvement on the rise side should render it possible to measure ten times faster binding reactions. This improvement in the liquid exchange rate k_{Dsp} does however not relate to the association rate constant, since the association rate depends both on the association rate constant, sample concentration and dissociation rate constant. Furthermore, since the association rate constant (k_a) can be calculated from the dissociation rate constant (k_d) and the binding affinity (K_D), increased resolution of the binding phase is of less interest. The faster liquid exchange rate does however make it possible to measure binding rates at higher sample concentrations in situations when this is needed. It can also be advantageous in cases when equilibrium is difficult to reach, as the affinity can be calculated from measured association and dissociation rates. With the increased resolution it is also possible to carry out kinetic measurements at higher temperature for thermodynamic studies, as the reactions rates increases with increasing temperature.

5.3 FALL TIMES

In the PSI cell the rise time and fall times are of the same magnitude. Compared to Biacore S51 the fall times were slightly improved with the lane shift in the PSI cell. Considering the greater width of the PSI cell, having unchanged or slightly improved fall times is rather good. The small increase in average fall time for the sample flow rate 270 µl/min can be disregarded as the uncertainty in the fall time measurement of detector row 25 in PSI is large as displayed by the standard error bars in figure 12. A flow rate of 270 µl/min is not relevant for kinetic studies and was only included to study the rise and fall times for extreme values.

When the process of the stealth inject was reversed for the cut-down, the fall times rather increased than decreased. An explanation for this could be that with the normal cut-down, the buffer flow already has the right flow rate as it is switched over from the other flow cell with valve commands, whereas with the stealth process the buffer flow rate is increased from a low flow rate for the wash out. For the cut down, valve operation is faster than increasing the flow rate of the buffer pump. The reason for leaving the buffer flow on during the whole injection was to avoid possible mechanical disturbances from valve operations that could interfere when extracting kinetic information from the sensorgrams. The fall times of the stealth inject with a normal cut down procedure were not measured, as they ought to be the same as before (this was confirmed by a few random measurements).

With the normal cut down, some dispersion of the buffer occurs through backward diffusion in the buffer inlet. For very long injections it could be advantageous to use the stealth inject for the cut-down as it would give a considerable shorter time for backward diffusion. If for some reason, very pure buffer is needed for the cut down, the stealth inject procedure is a good alternative for the cut down.

5.4 VARIATIONS BETWEEN THE DETECTION SPOTS

The difference in rise and fall times observed between different spots with the normal inject in the Biacore S51 prototype is partly explained by the position of the detection spot relative the sample inlet. In the measurements made here, the sample inlet is closest to spot 1 and spot 2 is closest to the buffer inlet. The reference spot is positioned in the middle. This explains why the fall times are faster for spot 2 and the rise times faster for spot1.
At low flow rates the shortest rise time was observed for spot 1, but however, at higher flow rates the reference spot had the shortest rise time (see figure 14). A possible explanation for this could be that at low flow rates, the whole flow cell is not completely filled out and the fastest way for the flow is to go straightforward. At higher flow rates, the flow is fast enough to fill the whole flow cell, with the flow at the sides slowed down by the flow cell walls and the fastest way for the flow to travel will be in the middle.

Due to the velocity profile with zero flow rate close to the flow cell walls, a small change in flow rates will have a rather large effect on the liquid interface positioning near the flow cell walls, whereas it will have only a small effect in the middle. This can lead to difficulties using the detector rows close to the flow cell walls for

measuring spots, as in the stealth inject when positioning the liquid interface over detector row 16.

5.5 KINETIC DETERMINATION OF LOW-MOLECULAR WEIGHT COMPOUNDS

Despite the improved rise time with the PSI-cell, it was not possible to resolve the kinetics for any of the low-molecular analytes used here. The association rate constants are still too fast to be resolved. The improved rise time in the PSI cell with the lane shift and in the Y-cell with the stealth inject implies that on-rates approximately 10 times respectively 6 times faster can be resolved.

For low-molecular weight compounds the upper limit association rate constants that can be resolved is more likely to be limited by the mass transport rate than the liquid exchange rate. As the response is proportional to the mass of bound analyte, more molecules of low-molecular weight must bind in order to get a useful response level. This in turn requires higher immobilization levels, which has a negative effect on the balance between the mass transfer and binding rate [9]. To be able to resolve higher association rate constants, mass transport limitations will have to be overcome.

Although the kinetic rate constants of the analytes tested here could not be resolved, the assays showed that the concept with lane shifts in the PSI-cell can be used for kinetic analyses. With the improved rise time faster reactions can be measured. It is shown that it is possible to address the immobilized spot and the reference spot with the ligand flow in the PSI-cell and binding information is obtained. The sensorgrams were comparable to the sensorgrams from the kinetic analyses performed in parallel in the Biacore S51 prototype. The affinity constants can be determined from concentration series of the samples.

5.6 THE PSI CELL

With the PSI cell it was possible to improve the rise times with on average a factor 10, rendering it possible to resolve ten times faster interactions. Besides the improved kinetic performance, the PSI cell has several other advantageous features, being very general and flexible. With the PSI cell it is possible to both adjust the sample flow width and the position of the sample lane by adjusting the relative flow rates of the buffer flow and sample flow. This makes it possible to immobilize up to as many as 11 spots with different ligands in the flow cell with the present configuration of the optical system as shown in figure 22. The immobilization would be far easier to perform than in the currently used Y-cell, as the ligand flow can be directed to cover only the desired detection spot.

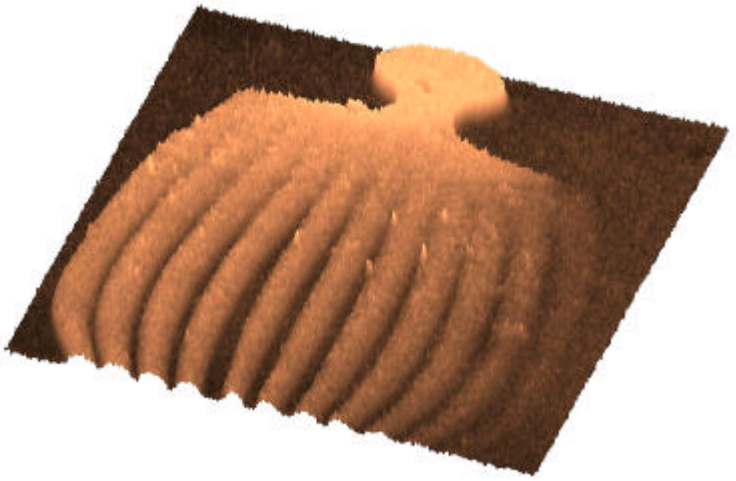

Figure 22 Picture taken with SPR microscopy showing 11 different immobilization lanes in the PSI cell. Picture kindly provided by Olof Andersson.

With the PSI cell it is also possible to performed gradient injections, giving different levels of immobilization.

5.7 FUTURE INVESTIGATIONS

Both the lane shift and stealth inject resulted in improved rise times, whereas the fall times were only slightly improved or unchanged. It is possible that the fall times can be improved by doing the switch from sample back to buffer differently. It was seen that valve operation was faster than pump operation. Perhaps the fall times with the PSI-cell can be improved if the cut-down is done using valve operation instead of adjusting the buffer flow rates. As the shift is done by changing the buffer flow rates, it could also be interesting to study the effect of the response rates of the buffer pumps on the rise and fall times, and if the shift can be done faster with faster pump response rates. In the experiments performed it was noticed that the two buffer pumps did not always react simultaneously, and it is possible that this time difference could give longer rise and fall times. Further studies or simulations are also needed in order to understand the velocity profile in the flow cell for low flow rates and high flow rates, explaining the different pattern seen in the fastest rise time with the normal inject in Biacore S51. Another feature of the lane shift that has not yet been studied is how the interface behaves during the shift. In these experiments a symmetric shift was used, with three detector rows separating the starting position with the detection position. It could be interesting to study if the dispersion increases if the distance of the shift is increased, and vice versa.

Further studies are also needed to understand the effect of the diffusion coefficient on the rise and fall times and to understand what the limiting factor of dissociation is. To improve the resolution of fast interactions other solutions such as miniaturisation and noise reduction should also be considered. With improved detector sensitivity and reduced mass transport effects faster association rate constants can be resolved.

6 CONCLUSIONS

The liquid exchange rate can be improved with new injection methods. The injection techniques for fast kinetics in this project, the lane shift and stealth inject, uses the principles of hydrodynamic addressing to position the sample in the flow cell clear of the detection spot before the injection start. In this way, the dead volume between the valve and flow cell is eliminated and sample dispersion is reduced, as the time for dispersion to occur is reduced to the time it takes to move the liquid interface across the flow cell at the injection start.

In the currently used Biacore S51, he rise time was improved with the stealth inject with on average a factor six. Reversing the process at the end of the injection did however not improve the fall times. A faster shift is obtained with valve operation instead of pump regulation. The reversed process of the stealth inject can however be advantageous to use for very long injections to minimize backward diffusion.

With the lane shift in the prototype flow cell PSI, the rise time was improved with on average a factor ten. The largest improvement was seen for low flow rates. The fall times were slightly improved or unchanged, compared to the Biacore S51. With the improved liquid exchange rate from buffer to sample seen for the lane shift, ten times faster association rates can be measured. Besides providing an increased resolution of binding phases, the concept of the PSI cell shows great potential and flexibility. By adjusting the relative flow rates, both width and position of the sample lane can be selected and it is possible to immobilize several different ligands in discrete lanes in the flow cell.

Despite the improved rise times it was not possible to determine any association rate constants of any of the low molecular drugs tested here. It should however be kept in mind that although a ten times faster liquid exchange rate means that ten times faster kinetics can be measured it does not directly relate to the resolution of the association rate constant. The association rate depends on the concentration, association rate constant and dissociation rate constant. The resolution of the association rate constant is more likely to be limited by mass transport than the liquid exchange rate. Since the resolution of the dissociation rate constant is limited by the liquid exchange rate and relates directly to the response seen during the dissociation phase, improved fall times would be of more useful. If the dissociation rate constant and affinity can be measured, the association rate constant can be calculated.

To further improve the resolution of fast interactions, other technical solutions such as increased detector sensitivity and noise reduction, and miniaturization should be considered.

7 ACKNOWLEDGMENTS

I would like to thank everyone at Biacore who has helped me during the time I have been working on this project. I would especially like to thank my supervisor Mattias Tidare for his guidance and support.

8 REFERENCES

1. MYSZKA, DAVID G. AND RICH, REBECCA L. (2000) Implementing surface plasmon resonance biosensors in drug discovery, PSTT 2000, 3(9), 310-317
2. www.biacore.com (Mars 2003)
3. KARLSSON, R. (1999) Affinity analysis of non-steady-state data obtained under mass transport limited conditions using BIAcore technology, J. Mol. Recognit. 1999, 12, 285-292
4. ROOS, H., MAGNUSSON, K. AND KARLSSON, R. (1995) Liquid handling system demands for kinetic analysis with optical evanescent field biosensors, Transducers 1995, 517-520
5. BIAtechnology Handbook (1998), Chapter 2, Realt-time BIA instrumentation, Chapter 3, Properties of the sensor chip surface, Chapter 4, The SPR signal, Chapter 5, Interpreting experimental data
6. BIACORE 3000 Instrument Handbook (2001), Chapter 2.1.4, Integrated µ-Fluidic Cartridge [IFC]
7. Biacore S51 Instrument Handbook (2001), Chapter D.3, Technical description, Flowcell, Chapter 2.3.3, Integrated µ-Fluidic Cartridge [IFC]
8. Verbal communication with Mattias Tidare, Biacore AB, Oct 2002- Mars 2003
9. KARLSSON, R., ROOS, H., FÄGERSTAM, L., AND PERSSON, B. (1994) Kinetic and concentration analysis using BIA technology, A companion to methods in Enzymology 1994, 6, 99-110
10. BIAapplication Handbook (1998), Chapter 4, Ligand immobilization chemistry, Chapter 5, Kinetic measurements
11. ROOS H. (2002) Aspects on Sensitivity in Biacore instruments, IM, Biacore AB.
12. TIDARE, M., ROOS, H. AND LINDBERG, U. Hydrodynamic addressing; a flow cell for improved signal quality in bioanalytical systems. Under construction.
13. D.J. TRITTON (1998) Physical Fluid Dynamics, second edition, Oxford Science Publications, Oxford.
14. Communication with Magnus Trovik, Biacore AB, 2003

APPENDIX

A CALCULATIONS OF REYNOLDS NUMBER

Reynolds number is described by

$$\mathrm{Re} = \frac{Vd_n}{n} = \left[d_n = \frac{2ab}{a+b}, n = \frac{h}{r}, V = \frac{q}{ab} \right] = \frac{2qr}{h(a+b)}$$

where V is the linear flow rate (m/s) and can be calculated by dividing the volumetric flow rate, q, with the cross section area ab. ν is the kinematic viscosity of the fluid, calculated by dividing the dynamic viscosity, η, with the density ρ (kg/m^3). For a rectangular shaped pipe, as the cross section of a flow cell, the hydraulic diameter equals 2ab/(a+b), where a and b is the length of the sides of the rectangle. For the flow channels and the inlets the hydraulic diameter will be the diameter of the pipe.

A density of 1000 kg/m^3 and the absolute viscosity for water 1002 μPa∗s was used for calculations of Reynolds number.

B NEW VALVE COMMANDS USED IN THE PSI CELL

The inlets are called 1, i and 2, where i is the middle inlet used for sample injection. 1 and 2 are used for buffer flow 1 and 2 respectively. The pumps are called d, b and c, where d corresponds to the dispensor (disp) pump used for sample injection, b buffer pump 1 and c buffer pump 2. Earlier combinations like "dn" and "di" for disp to needle and disp injection (direct inject) were preserved. Combinations like "b12" means that the buffer flow from pump 1 enters via inlet 1 and leaves the flow cell via inlet 2. The valves are numbered from 1-12 and a minus sign in front of the valve number is used to represent a closed valve.

Commands:

1) psi_di_b1_c2 -1,-2,-3,-4,5,6,-7,8,9,10,11,-12
   Sample injection through inlet i and buffer flow 1 and 2 in inlet 1 and 2 respectively
2) psi_dn_b1_c2 -1,-2,-3,4,5,6,-7,8,-9,10,11,-12
   Disp against needle and buffer flow 1 in inlet 1 and buffer flow 2 in inlet 2
3) psi_dn_b12_c2n -1,-2,3,4,5,6,-7,8,-9,-10,11,-12
   Wash: Buffer flow 1 enters through inlet 1 leaves through inlet 2. Buffer flow 2 (c) is passed by inlet 2 (never enters) and leaves through the needle.
4) psi_dn_b1i_c2i -1,-2,3,-4,5,6,-7,8,-9,10,11,-12
   Wash: Buffer flow 1 enters in inlet 1, buffer flow 2 in inlet 2 and both buffer flows leaves through inlet i.
5) psi_dn_bi1_c21 1,-2,3,4,5,-6,-7,-8,-9,10,11,-12
   Wash: Buffer flow 1 in via inlet i, out via inlet 1. Buffer flow 2 in via inlet 2, out via inlet 1.
6) psi_dn_bi1_c2n 1,-2,3,4,5,-6,-7,-8,-9,-10,11,-12
   Wash: Buffer flow 1 in via inlet i, out via inlet 1, buffer flow 2 passes by inlet 2 without entering and on towards the needle.
7) psi_dn_bin_c2n 1,-2,3,-4,5,-6,-7,8,-9,-10,11,-12
   Wash: Buffer flow 1 passes by inlet i (never entering) and leaves through the needle, buffer flow 2 passes by inlet 2 but does not enter and leaves through the needle.
8) psi_dn_bn_cn -1,-2,3,4,5,6,7,-8,-9,10,-11,-12
   Both buffer flows and the disp is directed against the needle.

C RISE AND FALL TIMES FOR THE LANE SHIFT 10 REPLICAS

Stigtider

Flöde	Spot		1	2	3	4	5	6	7	8	9	10	Average	STDEV
5 ul/min	r	s	0,492	0,5	0,531	0,545	0,553	0,619	0,633	0,658	0,665	0,698	**0,5894**	**0,074**
		ul	0,041	0,042	0,044	0,045	0,046	0,052	0,053	0,055	0,055	0,058	**0,0491**	**0,006**
	25	s	0,567	0,573	0,59	0,598	0,599	0,615	0,617	0,629	0,65	0,669	**0,6107**	**0,032**
		ul	0,047	0,048	0,049	0,05	0,05	0,051	0,051	0,052	0,054	0,056	**0,0508**	**0,003**
10 ul/min	r	s	0,245	0,247	0,248	0,249	0,256	0,256	0,259	0,259	0,262	0,263	**0,2544**	**0,007**
		ul	0,041	0,041	0,041	0,042	0,043	0,043	0,043	0,043	0,044	0,044	**0,0425**	**0,001**
	25	s	0,281	0,296	0,296	0,301	0,301	0,309	0,314	0,317	0,342	0,342	**0,3099**	**0,02**
		ul	0,047	0,049	0,049	0,05	0,05	0,052	0,052	0,053	0,057	0,057	**0,0516**	**0,003**
30 ul/min	r	s	0,134	0,134	0,137	0,145	0,148	0,149	0,149	0,163	0,167	0,17	**0,1496**	**0,013**
		ul	0,067	0,067	0,069	0,073	0,074	0,075	0,075	0,082	0,084	0,085	**0,0751**	**0,007**
	25	s	0,144	0,145	0,145	0,151	0,158	0,163	0,164	0,164	0,164	0,171	**0,1569**	**0,01**
		ul	0,072	0,073	0,073	0,076	0,079	0,082	0,082	0,082	0,082	0,086	**0,0787**	**0,005**
60 ul/min	r	s	0,095	0,097	0,097	0,099	0,1	0,107	0,109	0,114	0,118	0,126	**0,1062**	**0,01**
		ul	0,095	0,097	0,097	0,099	0,1	0,107	0,109	0,114	0,118	0,126	**0,1062**	**0,01**
	25	s	0,099	0,1	0,103	0,111	0,117	0,121	0,122	0,123	0,124	0,147	**0,1167**	**0,014**
		ul	0,099	0,1	0,103	0,111	0,117	0,121	0,122	0,123	0,124	0,147	**0,1167**	**0,014**
90 ul/min	r	s	0,073	0,074	0,074	0,074	0,075	0,083	0,091	0,094	0,098	0,099	**0,0835**	**0,011**
		ul	0,11	0,111	0,111	0,111	0,113	0,125	0,137	0,141	0,147	0,149	**0,1255**	**0,016**
	25	s	0,096	0,096	0,096	0,097	0,097	0,098	0,099	0,1	0,1	0,118	**0,0997**	**0,007**
		ul	0,144	0,144	0,144	0,146	0,146	0,147	0,149	0,15	0,15	0,177	**0,1497**	**0,01**
270 ul/min	r	s	0,049	0,05	0,054	0,055	0,071	0,073	0,073	0,073	0,074	0,075	**0,0647**	**0,011**
		ul	0,221	0,225	0,243	0,248	0,32	0,329	0,329	0,329	0,333	0,338	**0,2915**	**0,05**
	25	s	0,047	0,058	0,07	0,07	0,07	0,071	0,071	0,071	0,071	0,195	**0,0666**	**0,008**
		ul	0,212	0,261	0,315	0,315	0,315	0,32	0,32	0,32	0,32	0,878	**0,2998**	**0,038**

Falltider

Flöde	Spot		1	2	3	4	5	6	7	8	9	10	Average	STDEV
5 ul/min	r	s	0,31	0,312	0,314	0,319	0,322	0,325	0,339	0,341	0,343	0,349	**0,3274**	**0,014**
		ul	0,026	0,026	0,026	0,027	0,027	0,027	0,028	0,028	0,029	0,029	**0,0273**	**0,001**
	25	s	0,306	0,309	0,32	0,321	0,333	0,333	0,336	0,337	0,341	0,342	**0,3278**	**0,013**
		ul	0,026	0,026	0,027	0,027	0,028	0,028	0,028	0,028	0,028	0,029	**0,0275**	**0,001**
10 ul/min	r	s	0,195	0,2	0,207	0,21	0,213	0,217	0,217	0,218	0,219	0,223	**0,2119**	**0,009**
		ul	0,033	0,033	0,035	0,035	0,036	0,036	0,036	0,036	0,037	0,037	**0,0354**	**0,001**
	25	s	0,193	0,195	0,196	0,203	0,203	0,203	0,212	0,212	0,219	0,228	**0,2064**	**0,011**
		ul	0,032	0,033	0,033	0,034	0,034	0,034	0,035	0,035	0,037	0,038	**0,0345**	**0,002**
30 ul/min	r	s	0,103	0,104	0,113	0,113	0,119	0,12	0,124	0,124	0,125	0,133	**0,1178**	**0,01**
		ul	0,052	0,052	0,057	0,057	0,06	0,06	0,062	0,062	0,063	0,067	**0,0592**	**0,005**
	25	s	0,098	0,105	0,108	0,11	0,11	0,111	0,116	0,121	0,122	0,146	**0,1147**	**0,013**
		ul	0,049	0,053	0,054	0,055	0,055	0,056	0,058	0,061	0,061	0,073	**0,0575**	**0,007**
60 ul/min	r	s	0,075	0,08	0,091	0,092	0,093	0,093	0,095	0,095	0,096	0,096	**0,0906**	**0,007**
		ul	0,075	0,08	0,091	0,092	0,093	0,093	0,095	0,095	0,096	0,096	**0,0906**	**0,007**
	25	s	0,074	0,075	0,075	0,084	0,084	0,088	0,09	0,093	0,094	0,098	**0,0855**	**0,009**
		ul	0,074	0,075	0,075	0,084	0,084	0,088	0,09	0,093	0,094	0,098	**0,0855**	**0,009**
90 ul/min	r	s	0,072	0,072	0,072	0,072	0,073	0,074	0,083	0,084	0,085	0,09	**0,0777**	**0,007**
		ul	0,108	0,108	0,108	0,108	0,11	0,111	0,125	0,126	0,128	0,135	**0,1167**	**0,011**
	25	s	0,073	0,073	0,073	0,08	0,084	0,086	0,089	0,092	0,097	0,099	**0,0846**	**0,01**
		ul	0,11	0,11	0,11	0,12	0,126	0,129	0,134	0,138	0,146	0,149	**0,1272**	**0,015**
270 ul/min	r	s	0,049	0,049	0,049	0,05	0,063	0,067	0,067	0,074	0,074	0,079	**0,0621**	**0,012**
		ul	0,221	0,221	0,221	0,225	0,284	0,302	0,302	0,333	0,333	0,356	**0,2798**	**0,054**
	25	s	0,069	0,075	0,075	0,075	0,098	0,117	0,124	0,132	0,149	0,225	**0,1139**	**0,048**
		ul	0,311	0,338	0,338	0,338	0,441	0,527	0,558	0,594	0,671	1,013	**0,5129**	**0,216**